IDO-14443
Chemistry-Separation Processes
for Plutonium and Uranium
TID-4500 (13th Ed. Revised)

TECHNICAL PROGRESS REPORT FOR JANUARY THROUGH MARCH 1958 IDAHO CHEMICAL PROCESSING PLANT

C. E. Stevenson

September 15, 1958

AEC RESEARCH AND DEVELOPMENT REPORT

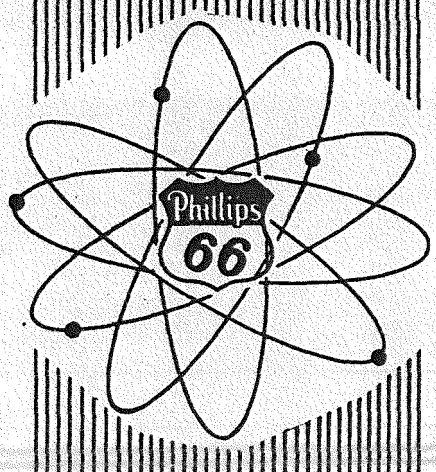

PHILLIPS PETROLEUM CO.
ATOMIC ENERGY DIVISION
(UNDER CONTRACT NO. AT (10-1)-205)
IDAHO OPERATIONS OFFICE
U.S. ATOMIC ENERGY COMMISSION

PRICE $2.25

Available from the
Office of Technical Services
U. S. Department of Commerce
Washington 25, D. C.

LEGAL NOTICE

TECHNICAL PROGRESS REPORT FOR JANUARY THROUGH MARCH 1958 IDAHO CHEMICAL PROCESSING PLANT

C. E. Stevenson

Including Contributions From

D. G. Reid
R. C. Shank

Previous Reports in This Series:

IDO-14324	IDO-14385
IDO-14337	IDO-14391
IDO-14350	IDO-14400
IDO-14354	IDO-14410
IDO-14362	IDO-14419
IDO-14364	IDO-14422
IDO-14383	IDO-14430

PHILLIPS PETROLEUM COMPANY
Atomic Energy Division
AT(10-1)-205

IDAHO OPERATIONS OFFICE
U. S. ATOMIC ENERGY COMMISSION

TABLE OF CONTENTS

(continued)

TABLE OF CONTENTS (continued)

LIST OF TABLES

LIST OF FIGURES

TECHNICAL PROGRESS REPORT FOR JANUARY THROUGH MARCH, 1958 IDAHO CHEMICAL PROCESSING PLANT

TECHNICAL BRANCH

C. E. Stevenson, Technical Director
D. M. Paige, Section Head, Chemical Engineering
C. M. Slansky, Section Head, Chemical Development
F. M. Warzel, Section Head, Process Engineering

Including contributions from

OPERATIONS BRANCH, D. G. Reid, Production Manager
R. C. Shank, Analytical Laboratory Supervisor

I. SUMMARY

Recovery of enriched uranium from a Zircaloy fuel composition was successfully accomplished in plant operation by the hydrofluoric acid dissolution process. Adequate first cycle and overall decontamination were achieved with low losses. Flowsheet modifications aimed to increase process capacity were studied. After 13 months' exposure at ambient temperature, corrosion of waste storage tank material was found to be less than anticipated.

In TBP-Hexone processing of aluminum alloy fuels, process performance was satisfactory with recycle of second and third cycle raffinates for use as first cycle scrub. Waste volumes were significantly reduced by this means. Initial difficulty with plutonium contamination of the uranium product was overcome by stabilizing column operation, reducing acid carry-over to the second cycle, and adding ferrous ion as a third cycle reductant.

Corrosion studies indicated the use of titanium for aluminum nitrate concentration was satisfactory, and that this material would adequately resist plant decontamination reagents. Studies of mild steel corrosion by neutralized aluminum nitrate wastes were initiated.

Validity of a parabolic rate law for aluminum dissolution in nitric acid was confirmed in laboratory studies. The continuous dissolver equation was tested with pilot plant data.

In the development of new and modified zirconium alloy processes, it was determined that the hydrofluoric acid process could tolerate an increased percentage of uranium in the feed by increasing nitric acid usage. The feasibility of this modification from the corrosion standpoint

will be determined. It appears that increased first cycle extraction capacity for such a process could be obtained by using TBP process equipment provided for aluminum fuels. Electrochemical studies indicated that the rate of dissolution of zirconium in nitric-hydrofluoric acid mixtures was controlled by the diffusion of hydrofluoric acid to the metal surface. Zircaloy-2 dissolved in such acid mixtures at substantially the same rate as zirconium, although in concentrated nitric acid tin was precipitated. The composition and stability of zirconium fluoride hydrates in equilibrium with nitric acid was determined. Conditions governing the TBP extraction of zirconium from nitrate and nitrate-fluoride systems were developed.

A process uranium monitoring instrument was placed on test. Wear tests of graphite bearings in canned rotor pumps were continued and tests of ceramic bearings are planned.

In studies of the fluid bed calcination process for aluminum nitrate wastes, silica gel was found to be superior to stainless steel as an absorbent for volatilized ruthenium in respect to capacity and vapor decontamination at higher velocities. In removing alumina particles from calciner off-gas by venturi scrubbing, increasing scrub rates at low gas velocity was less effective in improving efficiency than at high gas velocity. Heat transfer coefficients were measured for heating of the calciner bed by direct-fired tubes under pressure. Construction of a NaK heating system for the 2-foot square calciner is well along. A substantial portion of fine calcined alumina particles was found to dissolve in nitric acid. About half of the cesium contained in calcined alumina was volatilized at 1000° C. The process design of the demonstration calcining facility was tentatively determined.

In other studies of forming solids from wastes, aluminum was quantitatively precipitated as the phosphate from dilute nitrate solution. Conditions for extraction of aluminum with acetylacetone were developed. A gel was formed with sodium silicate solution from zirconium contained in a nitric-hydrofluoric acid solution.

In studies of a neptunium sample with the surface ionization mass spectrometer, neptunium-237 was readily identified and a small peak attributed to neptunium-236 was noted. A spectrometric means of determining boron in polyethylene tape was developed. Satisfactory uranium emission spectra were obtained using a hollow cathode tube.

An analytical procedure for the determination of tin in zirconium-base alloys was devised. Neptunium was determined in plant process streams by TTA extraction. Neptunium was largely found in the first Hexone cycle raffinate. Determination of fluoride by pyrohydrolysis and alkalimetric titration was developed to yield a standard deviation of 0.9 percent. Analytical methods were also developed for determining nitrate, nitrite, and copper.

II. PLANT PROCESS AND RELATED STUDIES

Studies of plant processes included analysis of results of recycling second and third cycle wastes as first cycle scrub, and of initial processing of Zircaloy-type fuel. Thirteen months' corrosion data on Type 316 ELC stainless steel in STR fluoride process waste are reported. Exhaustive tests are described on the use of titanium 75A in aluminum nitrate-nitric acid waste evaporators. Mild steel is being evaluated for use in storage tanks for caustic-neutralized ICPP first cycle aluminum wastes. Plant tests of iodine control by caustic and sulfite additions during waste evaporation were made.

A. Second and Third Cycle Aqueous Raffinate Recycle, J. R. Bower, Problem Leader; V. W. Irvine

Processing of enriched uranium from aluminum-uranium fuel elements by first cycle TBP extraction and later cycle Hexone extraction utilized the raffinate recycle flowsheet given in IDO-14422.

A buildup of plutonium in the first cycle, as indicated in IDO-14430 by analysis of the flowing stream samples, was confirmed from spot analysis of TBP first cycle product. Plutonium content was a factor of 2 to 10 times greater than that of first cycle feed, confirming its buildup and ultimate carryover into final product. Product analysis showed a plutonium content well above the desired value. The greatest activity occurred during a part of the run when excess acidity and column flooding from insufficient pulse energy were evident. When column rates were stabilized and acidity was properly adjusted, plutonium content of the product decreased indicating that most of the plutonium carryover was from one or both of these causes. With column rates stabilized at relatively low rates, the plutonium content of the product was reduced thirty-fold from the maximum previously experienced. Flowing stream samples taken at these column rates showed a plutonium decontamination factor of 10^5 for three cycles indicating the 0.05 molar phosphoric acid complexing agent was removing plutonium in the first cycle aqueous raffinate.

To give added protection against plutonium carryover into the final product, third cycle scrub was also adjusted to contain 0.05 molar ferrous ammonium sulfate and 0.10 molar sulfamic acid, as used in second cycle scrub. Product analysis obtained immediately preceding this addition showed an acceptable plutonium content. Plutonium content of the product was further reduced after the ferrous ammonium sulfate and sulfamic acid were included in the third cycle scrub. From all indications, with steady column operation and with acid concentrations within flowsheet specifications, the 0.05 molar phosphoric acid zirconium and plutonium complexing agent should remove enough plutonium to insure desired product purity without the addition of ferrous ammonium sulfate and sulfamic acid in the third cycle.

Average beta ratio of the final product (ratio of the specific activity of the product to the specific activity of unirradiated enriched uranium aged nine months) was 3.5 for a sustained period of plant operation using this flowsheet. Decontamination efficiency for fission products has been comparable to that obtained prior to adoption of the recycle flowsheet indicating that the many changes incorporated to increase throughput, decrease chemical usage and minimize waste volumes have not adversely affected the process.

Average decontamination efficiency for all three cycles, except for plutonium, is summarized below.

Log Decontamination Factors

	Total β	Total γ	Ion Chamber γ	Zr γ	Ru β	Nb γ
First Cycle	4.4	4.7	3.9	4.5	4.4	4.3
Second Cycle*	6.0	5.9	6.1	6.0	4.4	6.4
Third Cycle*	7.1	6.3	6.7	7.7	6.2	7.8

*Cumulative values.

Column losses for this flowsheet were comparable to those experienced prior to raffinate recycle. Cumulative column losses for the composited first cycle extraction and stripping columns were 0.10 percent and those for the composited second and third cycle raffinates, not recycled as scrub, were 0.007 percent. The first cycle losses were significantly above the design value of 0.01 percent maximum per column. Other column losses were within flowsheet design limits. Equipment malfunctions and operational difficulties during the first part of the run were largely responsible for the higher losses in the first cycle. Strip column losses for all cycles were negligible and were below design limits.

Further analysis of data obtained during processing of uranium-aluminum alloy type fuel in continuous dissolution equipment indicates that increased dissolution rates are obtained only at the expense of increases in catalyst requirements. Production of 1.55M aluminum dissolver solution, using 6.64N nitric acid dissolver feed, required 0.0165M mercuric nitrate catalyst in the dissolver feed at 50 percent dissolving capacity as compared with 0.0215M mercuric nitrate catalyst at full dissolving rate. Thus, doubling the dissolving rate required approximately one-third greater catalyst concentration.

Previous data(1) from dissolving other types of fuel indicated a catalyst saving of up to 75 percent when two dissolvers were used instead of one for processing irradiated uranium-aluminum fuel elements. Thus the present data confirm the possible savings in catalyst usage if dissolution is carried out at a lower rate in parallel equipment although it is apparent that different fuel elements may have different overall catalyst requirements.

(1) Rohde, K. L., Idaho Chemical Processing Plant TBP Process Performance July 1955 to May 1956, IDO-14397 (Secret)

B. Zircaloy Fuel Processing, J. R. Bower, Problem Leader; F. K. Wrigley

The first processing of a Zircaloy-type enriched uranium-zirconium fuel was completed during this quarter in the STR process. Tin contained in Zircaloy requires the use of a small amount of nitric acid in the latter part of the dissolving cycle. The specific activity of this core was markedly greater than that of the prototype core previously processed (IDO-14410, p. 13). The first cycle processing rate was increased considerably above the design value. The average first cycle decontamination factors were: gross beta, 3.42×10^3; gross gamma, 3.43×10^3; zirconium, 1.21×10^5; niobium, 7.52×10^4; and ruthenium, 2.06×10^2. The final product was satisfactorily reduced in activity.

It was found that the dissolution rate during the initial stage of dissolving was limited by the capacity of the off-gas system (dissolver pressurized). After the initial surge of off-gas, generally 20 minutes after the acid addition to the dissolver was started, the dissolution rate was limited by the capacity of the acid addition pump. It was possible with the present equipment to charge completely, dissolve, and remove from the dissolver a batch of metal in six to seven hours. The aqueous-to-organic flow ratio in the IA column was increased gradually to 8 : 1 during this run. The losses did not reach a detectable value until the column was run at a ratio of 7 : 1. At flow ratios of 7 and 8 the loss to the raffinate exceeded 0.1 percent in some instances. The latter part of the run was made with the IB column scrub and extractant flows reduced 40 percent. The change of flow ratio in the IA column and reduced flow to the IB column had little or no effect on decontamination. The supply of feed material was exhausted before the system could be adequately checked at the higher IA column flows.

Decontamination of cell equipment following operation was quite easy. The dissolver was simply flushed with water and the other equipment was given a 10 percent nitric acid flush followed by a water flush. A survey of the cells indicated a radiation background of 1.5 roentgen per hour in cell E (dissolution and feed adjustment) with a maximum reading of 6 roentgen per hour at the dissolver. The background in cell F (extraction) was 100 milliroentgen per hour.

C. Corrosion of Materials for STR Process High Activity Waste Storage, C. M. Slansky, Acting Problem Leader; T. L. Hoffman

Plant-type corrosion studies are being conducted on AISI Type 316 ELC and other grades of 18-8 Mo stainless steels while immersed in radioactive STR stored waste in tanks fabricated of Type 316 ELC welded with Type 315 filler wire.

Currently one of three 30,000-gallon vessels contains waste from processing zirconium and Zircaloy fuels by hydrofluoric acid dissolution (STR process). Four Type 304 sample jigs supported on cables through two different six-inch access riser heads accommodated the specimens.

The exposure period for the first sample removal was 13 months. The corrodent during the first 11 months was the processed waste from zirconium fuel processing, while the tank contained a composite waste from zirconium and Zircaloy processing for the remaining two months. Waste solution temperatures were about 25° C during this period although the cooling coils are designed to allow 57° C. The maximum corrosion occurred on two weld tabs which were prepared at the fabricating site using the process that was used to erect the vessel. This rate was 0.011 mils/month while on similarly exposed Type 316 ELC stressed hoops the rate was 0.003 mils/month. One Type 316 ELC stressed hoop specimen which was heat treated at 1250° F for one hour suffered 15 mil deep pits in the weld deposit. On the basis of these data the designed life of five years for these tanks can be extended significantly. The lowest specimen was located six inches from the bottom of the tank and upon removal showed no evidence that precipitates were being formed.

D. Titanium Waste Evaporator Tests, C. M. Slansky, Acting Problem Leader; T. L. Hoffman, O. R. Klemens

In the uranium-aluminum fuel recovery process at the ICPP, throughput is limited by the capacity of the headend and waste evaporators. Evaporator capacity can be increased by operating at higher steam pressures but the increased temperature is known to be prohibitive for the Type 347 stainless steel material. In re-designing the evaporator to include more tubes, new materials were also investigated. Data from Hanford and scoping studies here showed titanium as a likely improvement over Type 347 stainless steel.

These process evaporators are routinely required to handle solutions as listed in Table II-1.

Table II-1

Nominal Composition of Process Streams
Handled by the ICPP Headend and Waste Evaporators

Evaporator	Specific Gravity	Product Composition, M					
		Aluminum	Uranium	Nitrate	Acid	Mercury	Sodium
Headend	1.213	1.5	0.0088	5.58	1.08	0.005	0.10
Waste	1.420	2.3	--	8.38	1.33	0.008	0.15

Note: 0.06M phosphate may exist in these process streams.

A prototype single titanium tube evaporator was used to measure the corrosion rate of titanium immersed in a boiling reflux synthetic waste solution. This evaporator was composed of a titanium 75A bayonet-type heat exchanger which was surrounded by a Type 347 stainless steel shell and water-cooled condenser. Measured corrosion on

the titanium heat exchanger after six months' operation at 137° C under waste concentration conditions (no phosphate) was less than 0.01 mils per month. Evidence of grain boundary attack at either the welds or wrought areas was absent.

Occasionally, the evaporators must be decontaminated before personnel can perform maintenance work. Accordingly, the corrosion rate was measured on titanium under decontaminating procedures used in the plant for austenitic stainless steel vessels.

The previously described single tube evaporator was continuously exposed for three 62-hour cycles in the series of solutions shown in Table II-2.

Table II-2

Chemical Solutions Used in the Corrosion Studies of Titanium 75A Under Simulated Plant Decontamination Procedures

Decontamination Medium	Temperature Conditions	Time, Hours
10% Citric Acid	137°C - 35 psig	8
10% NaOH - 2.5% Tartaric Acid	"	8
10% HNO_3	"	8
10% Oxalic Acid	"	8
10% HNO_3	"	8
0.05M HNO_3 - 0.003M $H_5{}^{106}$	"	4
10% HNO_3	"	8
20% HNO_3 - 3% NaF	30°C - 0 psig	2
10% HNO_3	137°C - 35 psig	8
		62

The observed average cycle rate on the titanium heat exchanger was 0.016 ± 0.007 inches penetration per month. This confidence level was established by calculating the standard deviation of the observed rates for individual cycles. The cumulative rate as a function of the number of cycles (n) was found to be:

$$0.016\ (n) \pm 0.007\ n \text{ inches per month}$$

The prototype evaporator was later exposed for 90 days to synthetic aluminum nitrate waste containing 0.06M phosphoric acid, the latter being a process additive used for plutonium control. The acid was replaced every seven days with a freshly prepared acid solution. The evaporator was operated at 35-37 psig steam (127-132° C). A tenacious crystalline deposit of doubtful origin appeared on the exposed area of the titanium 75A bayonet-type heat exchchanger. Bright, metallic-looking spots were present under this deposit. Evidence of grain boundary attack at either the weld or wrought areas of the tube was absent. An exceedingly low

general corrosion rate was indicated from weight loss measurements--final weight was equal to the initial weight.

Severe intergranular corrosion (40 mil deep) was observed on the Type 347 stainless steel flange swage of the outer shell. Figure II-1 is a micrograph of the swage cross-section. The magnitude of this metallic destruction is further evidence for the desirability of replacing the austenitic stainless steel evaporators with a more suitable alloy.

A scaled-up evaporator was built to evaluate further welding problems and corrosion around the tube-tube sheet junctions. A five-tube thermosyphon evaporator was designed with seamless commercial grade titanium 55A as the material for the evaporator tubes and tube sheets. Surrounding the evaporator tubes is a carbon steel steam chest. The jackleg and disengaging section are fabricated from Type 347 stainless steel. Considering the outside diameter of the heat exchanger tubes, this evaporator has 2.76 square feet of heat transfer surface. Currently, this five-tube thermosyphon titanium evaporator is being operated under the waste evaporator conditions of Table II-1 with the addition of 0.05M phosphate.

Constant operation was achieved under 57 ± 2 psig steam chest pressure at a feed rate of about 7.5 gal/hour of 1.15 specific gravity feed. The resulting evaporation concentrates the solution to about 1.31 specific gravity. The evaporator has operated satisfactorily for two and one-half months and will be examined after six and twelve months of testing.

E. Caustic Neutralized Aluminum Nitrate Waste, C. M. Slansky, Acting Problem Leader; B. D. Withers

Caustic neutralization of first cycle aluminum nitrate wastes and subsequent storage in carbon steel tanks is an alternate to acid waste storage in stainless steel tanks. A corrosion experiment was initiated to obtain data on carbon steel exposed to neutralized ICPP aluminum waste.

A synthetic caustic-neutralized aluminum nitrate waste was prepared by adding first cycle waste composed of:

Aluminum Nitrate	1.95M
Nitric Acid	1.43M
Sodium Nitrate	0.09M
Mercuric Nitrate	0.006M
Phosphoric Acid	0.06M

to a 50 percent caustic solution. The amount of caustic used was 10 percent in excess of that amount required for neutralization to sodium aluminate. This solution was maintained at 60° C and stirred continuously to prevent settling of solids.

FIGURE II-1

CORROSION OF STAINLESS STEEL
IN ALUMINUM NITRATE EVAPORATION

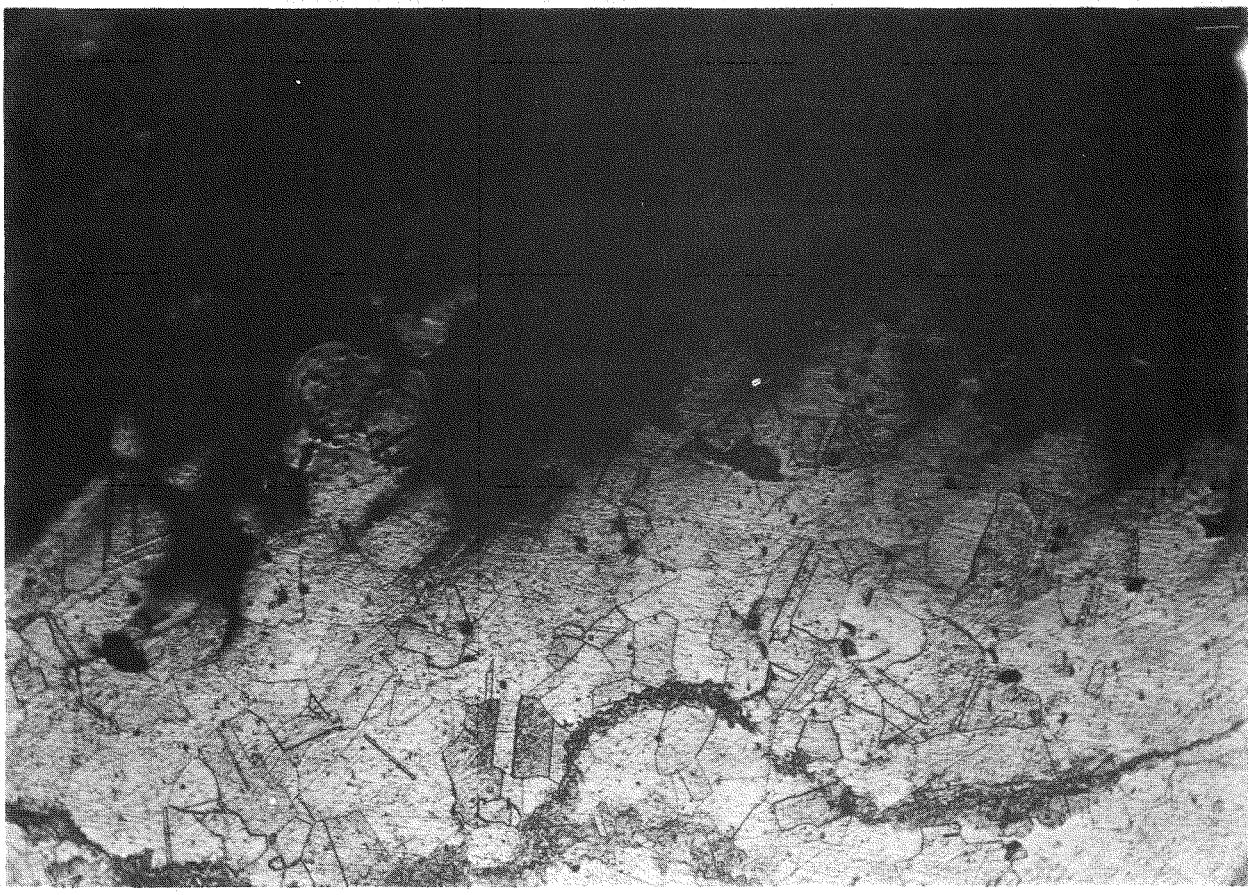

ETCH: AQUA REGIA 150X

TYPE 347 STAINLESS STEEL SHELL SWAGE CROSS SECTION FROM THE PROTOTYPE SINGLE TUBE EVAPORATOR

CPP-S-846

Welded 1020 carbon steel samples were exposed at the interface of this solution in the as-welded and stress relieved conditions. Samples stressed both below and beyond the yield point were exposed in the liquid phase.

Two as-welded and two stress relieved samples were removed after 90 days' exposure. All samples in the vapor phase and at the interface showed general pitting (10-15 mils deep) but no corrosion was observed on the liquid phase exposed samples. Weight loss measurements indicated an attack of one mil per year which corresponds qualitatively to the vapor phase pitting. The solution was found to be unstable and the solid phase separated was found to be crystalline aluminum hydroxide.

F. Iodine Control in Plant Equipment Waste Evaporation, J. R. Bower, Problem Leader; G. K. Cederberg

The laboratory data previously reported showed that process equipment waste solutions (PEW) which contain iodine can be treated to help hold the iodine in solution during concentration in an evaporator. Neutralization of acid PEW with caustic and the addition of sodium sulfite to the neutral mixture gave the greatest improvement.

Following a barium recovery run, the PEW iodine concentration approached the upper tolerable concentration limit. To counter this condition a series of plant tests was initiated to apply the laboratory findings. These tests substantiated the laboratory data that iodine is adequately retained in slightly basic solutions. They resulted in minimizing the number of batches of condensate which otherwise would have been recycled to the evaporator because of excessive iodine concentrations.

With no neutralization of the evaporator feed, there was essentially no decontamination from iodine-131 in the condensate. When the evaporator feed was neutralized with caustic (0.01 to 0.1M basic), the condensate iodine decontamination factors increased from 25 to 100 (feed to overhead) over five successive batches. The gradual increase is attributed to the gradual flushing of iodine-131 from the bubble cap column and the condenser and dilution of heels left in the condensate receiver after each transfer.

Adding sodium sulfite to a batch of basic feed to give 0.005M sodium sulfite feed solution yielded a condensate which contained about 0.5 percent of the iodine from the feed, giving an iodine decontamination factor of 200. This particular batch was produced following a caustic neutralized evaporation which gave an iodine-131 decontamination factor of 75. Thus these tests demonstrate that iodine in the PEW can be controlled by neutralization and, if further decontamination is required, the addition of sodium sulfite (0.005M) may approximately triple this decontamination.

The principal source of iodine-131 in the PEW appeared to be from the RaLa process off-gas lines which drain to the evaporator feed tank (WL-102). Iodine in excessive concentration does not necessarily come from solution transfer from RaLa equipment to the PEW collection tanks (WG-101 or WH-100). Analyses of the PEW solution in the collection tanks and in the feed tank after transfer indicate that the iodine-131 concentration varies between 10^3 and 10^4 d/(min)(ml) in the collection tanks and between 10^5 and 10^6 d/(min)(ml) in the feed tank. The rate at which iodine-131 builds up in the evaporator feed tank depends on the decay time since the last RaLa run and the number of RaLa solution transfers in the cell, which presumably stir up and volatilize the iodine in the cell.

Plant operation throughout the quarter encountered other batches of PEW with high iodine concentration but some of these coincided with conditions where vessels were being decontaminated with dilute caustic. This caustic in the PEW feed gave an adequate iodine decontamination during the evaporation and also improved the gross beta decontamination factor. For a six-day operating interval, during which time the PEW was basic from plant decontamination solutions, the beta decontamination factor during evaporation was 1.1×10^5, whereas it is usually 1.3×10^3.

The iodine decontamination factor was about 17. This is low compared to the test run decontamination factor of 25 to 100 but it is explainable by the fact that this was based on the iodine concentration of the feed before it received the stack drainage which is a major iodine contributor and was not sampled during the reference interval. The actual iodine decontamination factor was possibly in the range of 100 to 200.

III. ALUMINUM DISSOLUTION STUDIES

Development of a reaction rate equation for the mercury-catalyzed dissolution of aluminum is described. The theory of operation of a continuous dissolver was applied to pilot plant data.

A. Dissolution Rate Studies, H. Schneider, Problem Leader; R. F. Murray

Experimental work is currently under way to evaluate the terms in a reaction rate expression of the form

$$\frac{d\ (Al^{+++})}{dt} = \frac{k'}{(Al^{+++})}$$

describing the appearance of aluminum ion during dissolution in nitric acid using mercuric nitrate catalyst. The k' indicated in the expression is not a true constant, but is specific only for a given set of initial conditions. A value of k has been evaluated where

$$k' = f\ [k,\ \text{area},\ HNO_3,\ Hg(NO_3)_2]$$

for one-inch square specimens of 2S aluminum plate in one liter of solution. Using graphical techniques, an empirical expression has been developed in terms of initial concentrations which is valid for a given run.

The general rate expression in the integrated form is

$$\frac{(Al^{+++})^2}{2} = k'\ t + \text{constant}.$$

The constant of integration which is the induction period has shown no consistent pattern. Figures III-1 and -2 show plots of

$$\frac{(Al^{+++})^2}{2}$$

versus time for runs made at five initial nitric acid concentrations, and 5 levels of initial mercuric nitrate.

A logarithmic plot of initial nitric acid concentration versus k' in the range from 1 to 10M nitric acid shown in Figure III-3 follows a straight line with a slope of 1.0. The line has been drawn through the k' value for the 1M acid to insure greater accuracy for the intercept value which is very critical at acid concentrations near 1M although it will produce more error at higher acid values than an average line through the points.

Then

$$k' = (\ln 1.15\ HNO_3)_o.$$

FIGURE III-1
DISSOLUTION OF 2S ALUMINUM SHEET
IN MECURIC NITRATE CATALYZED
NITRIC ACID AT 88°C.

SYMBOL	NO. RUNS	INITIAL HNO_3, M	INITIAL Hg^{++} M
I △▲▲▲▲	4	5.0	5×10^{-3}
II ▲	1	5.03	7.8×10^{-4}
III ■	1	2.39	5×10^{-3}
IV ⊙●	2	0.98	5×10^{-3}

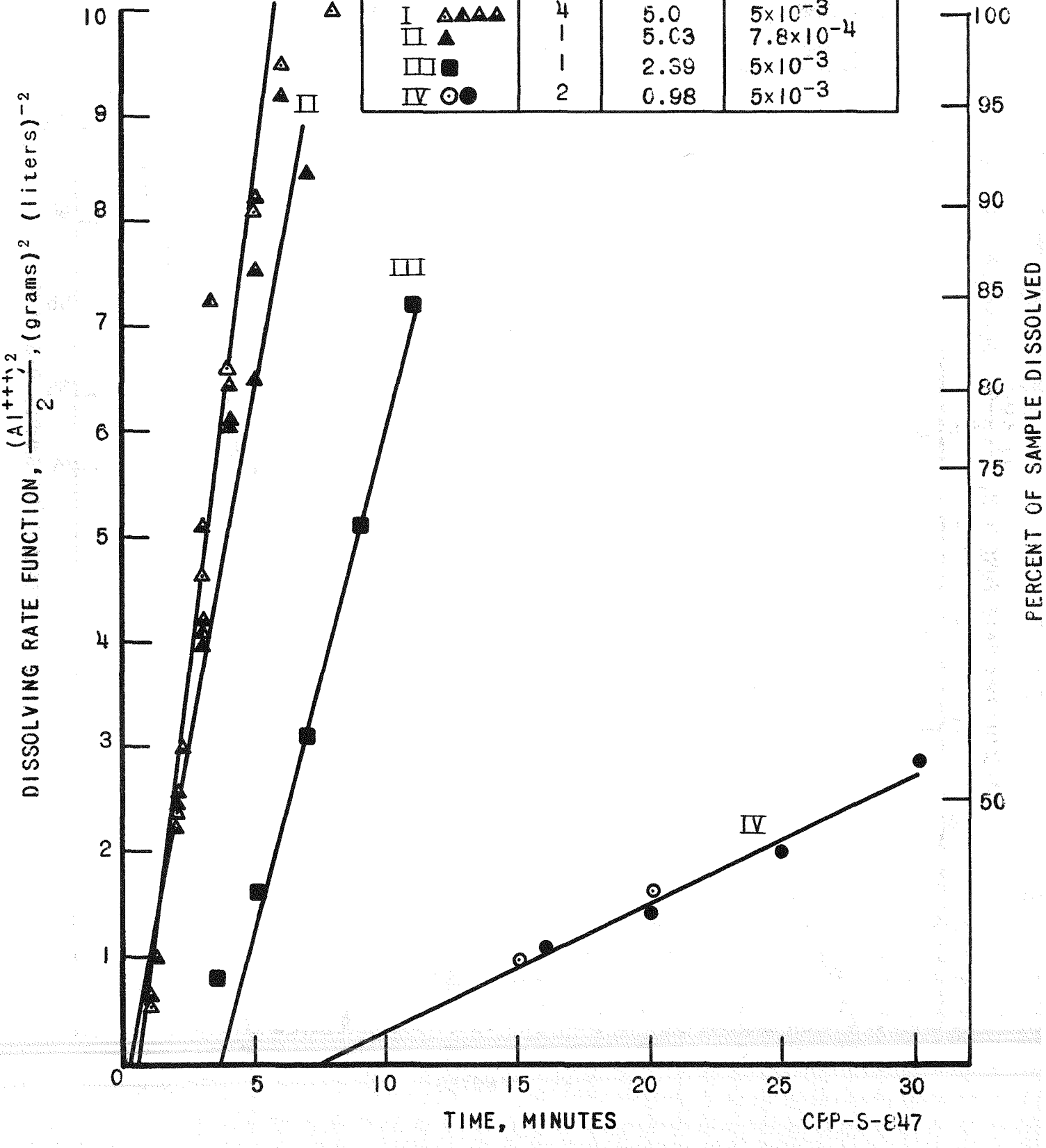

CPP-S-847

FIGURE III-2

DISSOLUTION OF 2S ALUMINUM SHEET IN MERCURIC NITRATE CATALYZED NITRIC ACID AT 88°C.

SYMBOL	NO. RUNS	INITIAL HNO_3 M	INITIAL Hg^{++}, M
I ⊙●	2	7.5	5×10^{-3}
II □■	2	10.0	5×10^{-3}

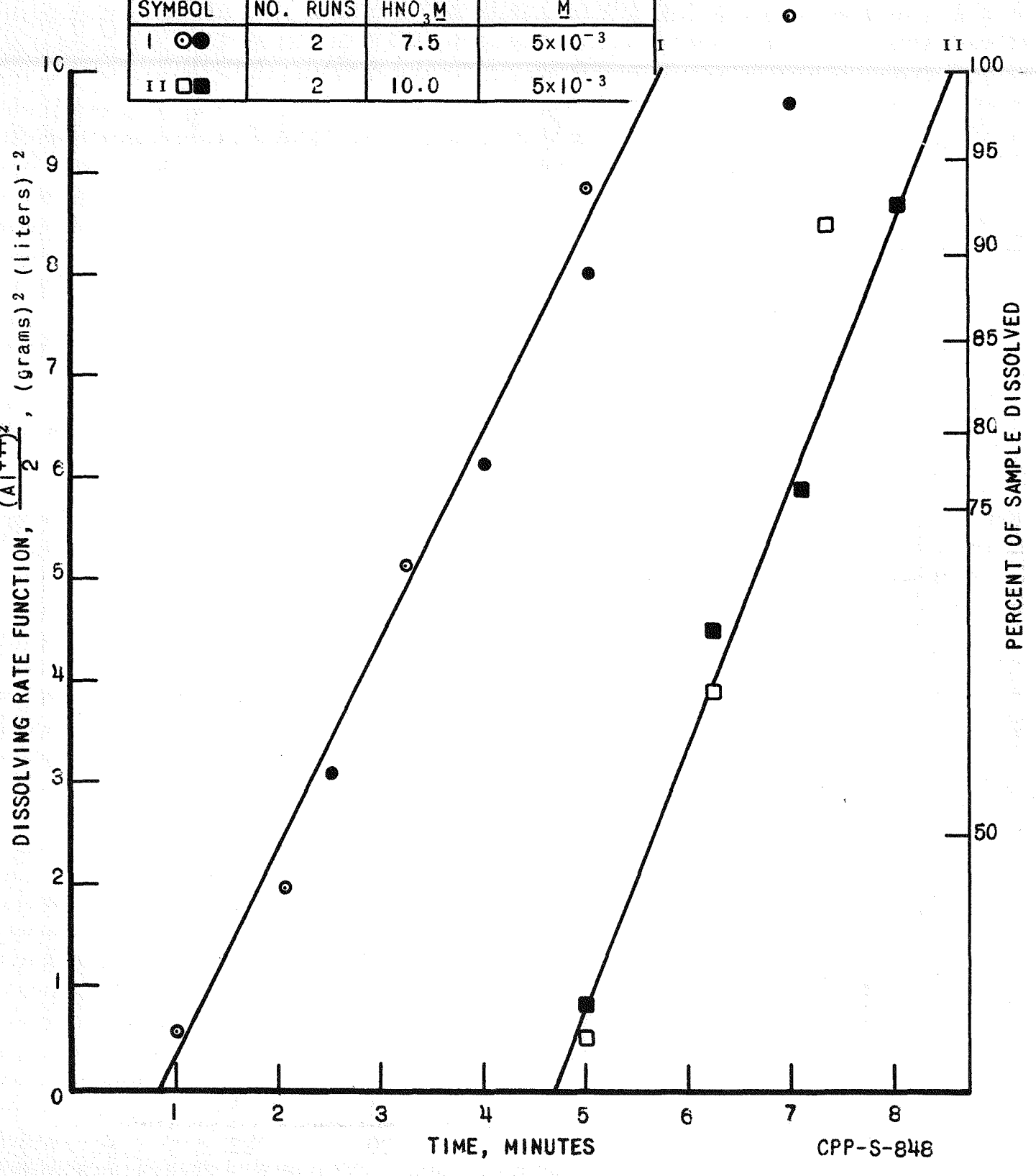

CPP-S-848

FIGURE III-3
REACTION RATE CONSTANT AS A FUNCTION OF INITIAL ACIDITY AT 5×10^{-3} M INITIAL $Hg(NO_3)_2$

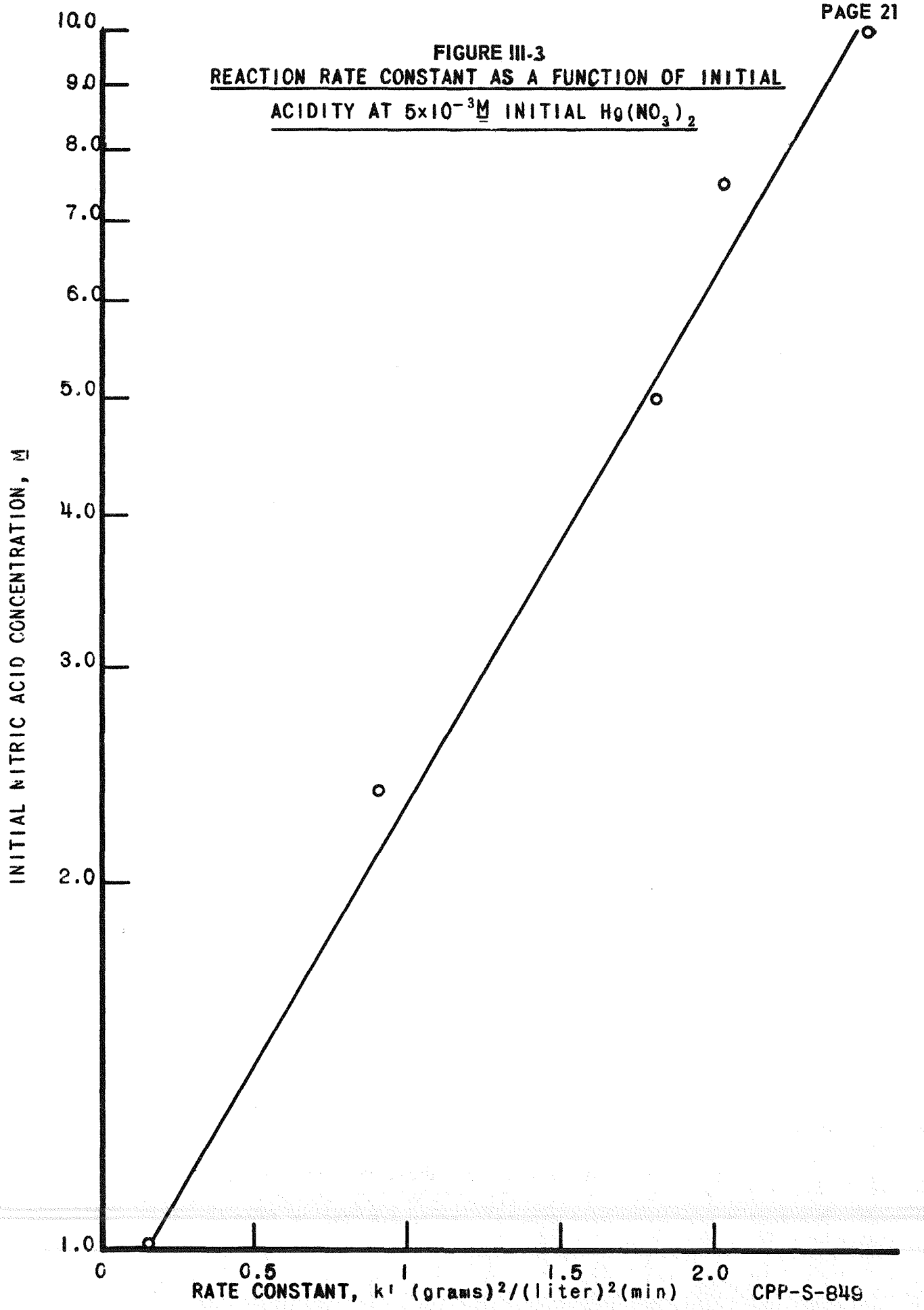

The value k' can be further defined as a function of initial area and initial mercuric nitrate concentration. A plot of ln k' versus ln initial mercuric nitrate for several runs at an initial nitric acid concentration of 5M is shown in Figure III-4. The correlation for k' values for cylinders extends over a wider range of mercuric nitrate concentration, but both the slopes are comparable. Using the slope of 0.17 for rectangles in the mercuric nitrate concentration range from 1 to 10 x 10^{-3}M with 5M initial acid

$$k' = 4.2 \left[Hg(NO_3)_2 \right]_o^{0.17}.$$

Now assume

$$k' = k(area)_o \, 4.2 \left[Hg(NO_3)_2 \right]_o^{0.17} \, (\ln 1.15 \, HNO_3)_o.$$

Then

$$K = \frac{k'}{(area)_o \quad 4.2 \left[Hg(NO_3)_2 \right]_o^{0.17} (\ln 1.15 \, HNO_3)_o}$$

$$= \frac{1}{(12.9)\,(4.2)\,(0.41)} = 0.0455 \; g^2 \, l^{0.83} \, moles^{-0.83} \, cm^{-2}.$$

The area term is treated as a constant directly proportional to the initial geometric area. This has been done for the present because the actual area during dissolution cannot readily be determined. The assumption of constant area must be made to separate the mercury and acid effects. Otherwise a product term involving area and either acid or catalyst would have to be treated as a single variable.

Then the empirical rate expression describing aluminum dissolution in mercuric nitrate catalyzed nitric acid for otherwise constant conditions is

$$\frac{d\,(Al^{+++})}{dt} = \frac{(4.55 \times 10^{-2})\,(area)_o\,(\ln 1.15\, HNO_3)_o\,\left[Hg(NO_3)_2 \right]_o^{0.17}}{(Al^{+++})}$$

Where

(Al^{+++}) = aluminum dissolved, g/l
$(area)_o$ = initial area, cm^2
$(\ln 1.15\, HNO_3)_o$ = $\log_e$ initial HNO_3, M
$\left[Hg(NO_3)_2 \right]_o$ = initial $Hg(NO_3)_2$, M

This holds at 88° C and initial $HNO_3 \geq 1$, assuming area dependence is zero order.

It must be emphasized that the above rate expression was evaluated under specific conditions. Experimental work is continuing to extend the range of conditions so a general expression can be formulated.

FIGURE III-4

REACTION RATE CONSTANT AS A FUNCTION OF INITIAL MERCURIC NITRATE CONCENTRATION

INITIAL NITRIC ACID CONCENTRATION: 5.0 M

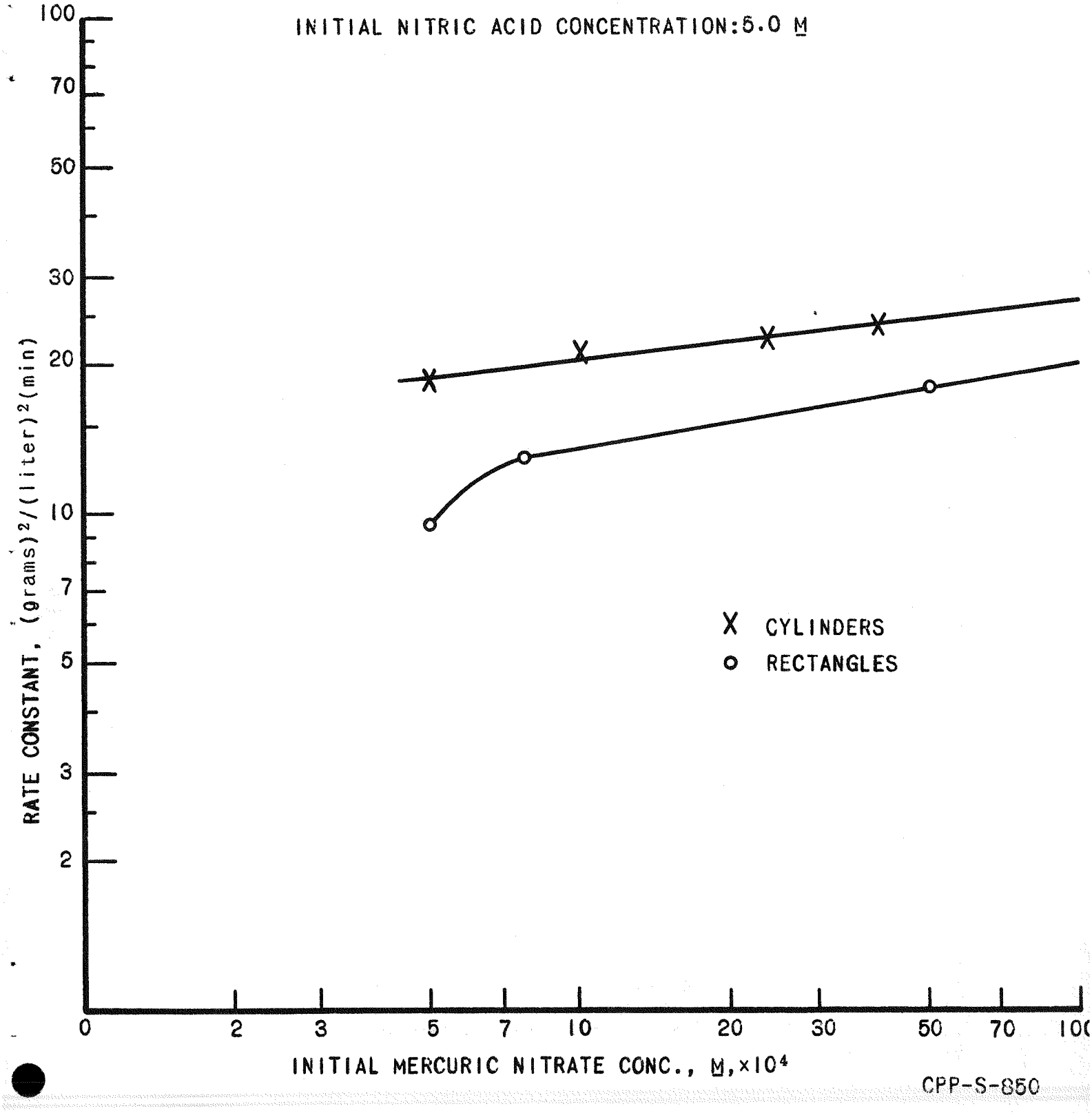

CPP-S-850

B. Continuous Dissolver Theory, H. Schneider, Problem Leader; E. E. Erickson

A continuous dissolver equation for a first order reaction rate was reported in IDO-14430. This equation has been applied to the continuous dissolution of aluminum in nitric acid to predict the trends in dissolution rate with changes in geometric shape of slugs and dissolvent flow rate. The predicted trends were compared with the pilot plant data of Boeglin and Buckham for a 2-inch dissolver(2).

The geometric shapes investigated by Boeglin and Buckham fall into two classes: (1) rods, in which the significant attack may be considered to be two-dimensional; i.e., the change in length during dissolution may be neglected, and (2) thin plates, tubes, and flattened tubes, in which the attack may be considered to be one-dimensional; i.e., the thickness is the only dimension that changes significantly.

From the continuous dissolver equation, general curves for dissolution rate as a function of liquid flow rate were calculated for the two above cases. An initial acid concentration of 5.6M nitric acid and a stoichiometric ratio of 3.88 moles acid consumed per mole of aluminum dissolved were assumed. The dissolution curves are given in Figure III-5. Note that the dissolution rate and flow rate are related to the product concentration, so that the slope of the curve depends on the product concentration.

The curves have no significance numerically as they stand. However, by assuming reaction rate constants for the various shapes to be the same under the same acid and catalyst conditions, and by using the packing factors (i.e., 1-void fraction) measured by the above authors, and physical dimensions of the initial fuel shapes in the dissolver equation, ratios of dissolution rates for the various shapes were established.

Theory predicts that, at higher reaction rates, the shape of the fuel element being dissolved would not affect the dissolution rate, while at lower catalyst concentrations, the shape would influence the rate quite strongly. The data are in close agreement with the theory.

The significance of the results can be explained graphically. Consider a plot of the total rate of dissolution versus the column height for two catalyst concentrations, A and B, as indicated in Figure III-6. The acid feed rate is held constant. The rate increases as the height increases, levelling off when the acid is consumed and as the reaction velocity decreases to a very low value. A point "a" is reached, at catalyst concentration "A", at which the rate becomes essentially constant, and additional height is ineffective in increasing this rate.

(2) Boeglin, A. F. and Buckham, J. A., Effect of Geometrical Shape on the Continuous Dissolution of Aluminum in Mercury-Catalyzed Nitric Acid, IDO-14425, December 31, 1957 (Unclassified)

FIGURE III-5

GENERAL DISSOLUTION RATE CURVES FOR
TWO CLASSES OF FUEL ELEMENT SHAPES

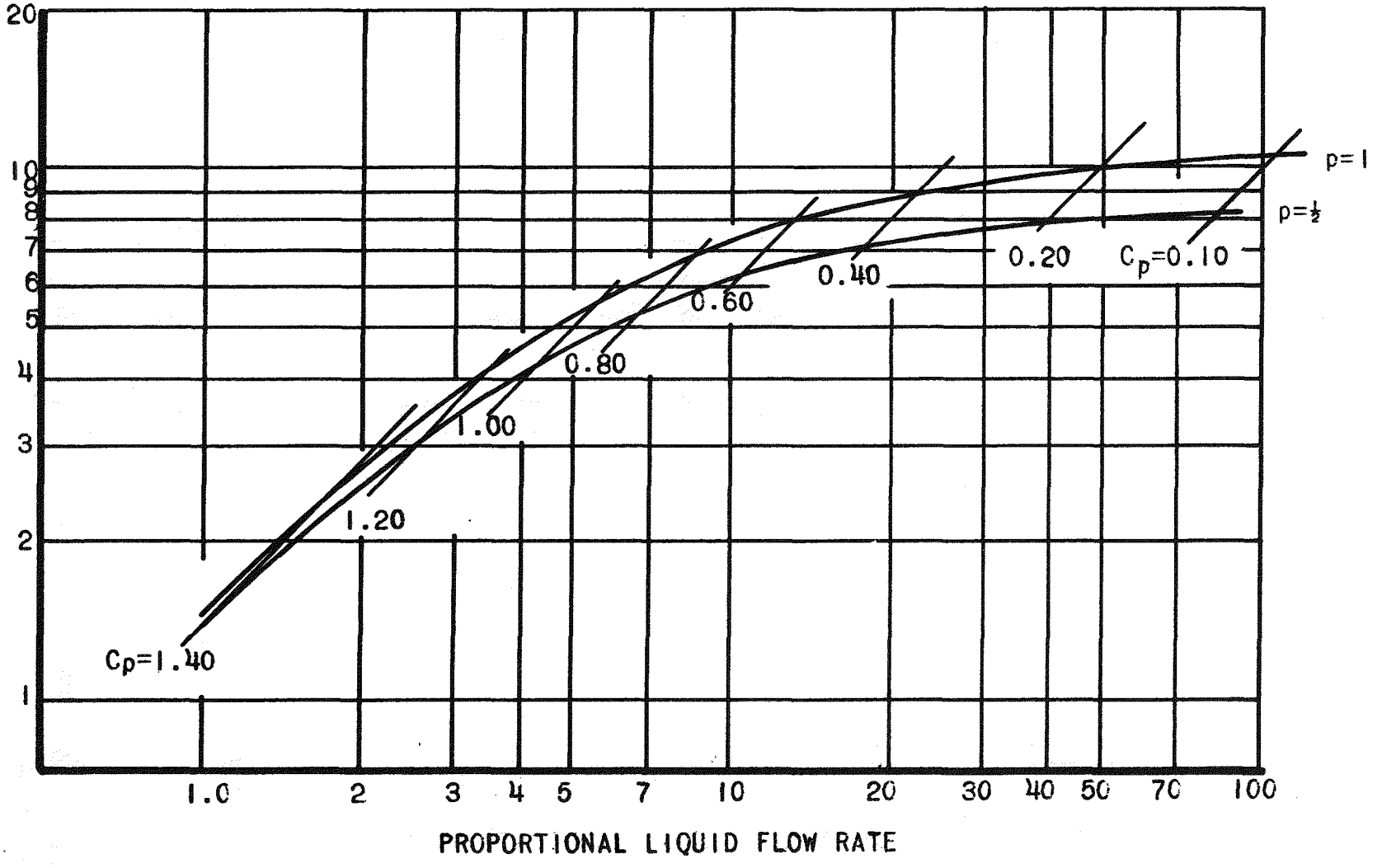

Figure III-6

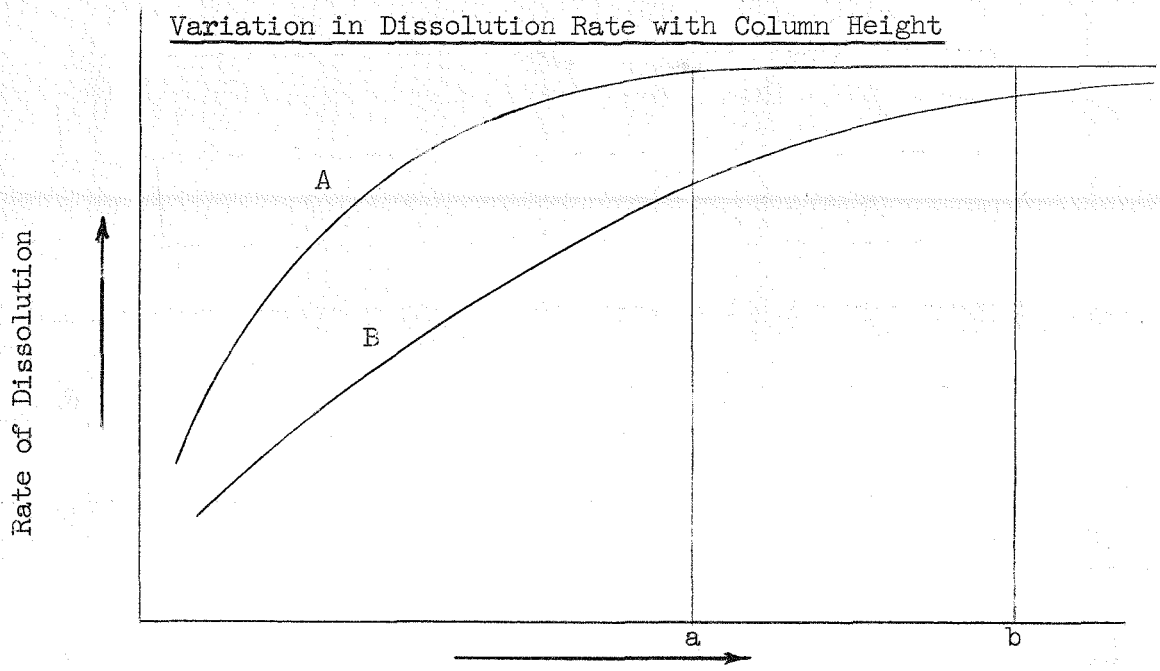

The height axis may also be considered to be a surface area axis. Suppose that the column is operating at catalyst concentration "A" with round rods, at or beyond point "a". If slugs of another shape, with a greater surface area, are put in the column, the dissolver will operate further out on the curve, say at "b". Thus, essentially no increase in rate of dissolution will occur. However, if catalyst concentration "B" is used, the lower reaction velocity allows an increase in surface area, through an increase in column height or a change in fuel shape, to give an increase in rate of dissolution.

The dissolver equation used with the available physical measurements predicted that rods and tubes would dissolve at nearly the same rate at lower catalyst concentration. Plates and flattened tubes also should dissolve at similar rates, but at a higher level than the rods and tubes--up to about 2.5 times higher. This also is substantially in agreement with the available data.

IV. DEVELOPMENT OF PROCESSES FOR ZIRCONIUM FUELS

The existing recovery process for zirconium-uranium fuels is a hydrofluoric acid headend process. The capacity of the installed equipment is probably inadequate for future needs. Research and development efforts are directed toware three goals, (1) modification of the hydrofluoric acid process flowsheet to enable the processing of fuels of higher uranium content at a somewhat higher rate, (2) re-arrangement and combination of ICPP processing facilities to obtain a much higher processing rate with an STR-type process, and (3) development of an entirely new, optimum process for zirconium fuels which would accommodate a wide range of compositions at adequate and economical rates. These studies are being completed for both short and long range needs. The optimum flowsheet development is proceeding with basic studies on the nitric-hydrofluoric acid system relative to dissolution kinetics, phase studies, and macro zirconium extraction. Pilot plant equipment is being constructed for continuous zirconium dissolution studies.

A. STR Flowsheet Modifications, K. L. Rohde, Problem Leader; O. W. Parrett, C. E. May

The present hydrofluoric acid zirconium fuel (STR) process[3,4] has two major limitations: (1) uranium tetrafluoride will precipitate during dissolution if much more than one percent uranium is contained in the overall fuel composition(meat alloy, cladding, and structural material); and (2) the waste storage cost is high because the corrosive and voluminous first cycle aqueous raffinate is stored without concentration.

It has been found that the use of a second dissolution step, either by making the hydrofluoric acid dissolver solution 1M in nitric acid and digesting for one hour or by decanting the dissolver solution and treating the uranium tetrafluoride residue with 1M nitric acid, will produce complete dissolution of fuel assemblies containing up to 3 percent uranium in zirconium or Zircaloy-2. The former treatment, which is an extension of the Zircaloy modification of the original flowsheet, appears more acceptable. The results of a series of dissolutions of 2 and 3 percent uranium fuels are shown in Table IV-1. The dissolver solution nitrate concentration, the adjusted feed composition and the distribution of uranium between solution and residue are shown. The feasibility of obtaining a homogeneous dissolver solution is shown by experimental dissolutions 5 and 6. In support of this work a few scoping studies were made using the residue from dissolution 3. Weighed aliquots of the residue were

(3) Jonke, A. A., Munnecke, V. H., Vogel, R. C., and Vogler, S., Process for Recovering Fuel from the Mark I Submarine Thermal Reactor, ANL-5242, February 24, 1954 (Confidential).

(4) Leek, C. B., Lemon, R. B., and Wrigley, F. K., Processing Uranium-Zirconium Alloy Reactor Fuel Elements, presented at the 4th Nuclear Engineering and Science Congress, March, 1958.

Table IV-1

Modified Hydrofluoric Acid Dissolution
of 2 and 3 Percent Uranium-Zirconium Alloys

Hydrofluoric acid addition and dissolution - 5 hours
Nitric acid digestion for uranium oxidation - 1 hour

Experiment No.	Uranium Content of Fuel, Percent	Nitrate in Dissolver Solution, M	Weight of Dissolver Residue, Mg	Complexed Feed Solution Composition				Uranium Distribution		
				Zr M	F M	H M	U G/L	Solution Gm	Residue Gm	Total Gm
1	1.92	0.02	100	0.59	3.5	1.2	1.07	2.84	0.06	2.90
2	1.96	0.02	341	0.52	3.5	1.4	0.91	2.73	0.20	2.93
3	2.84	0.02	4680	0.53	3.8	1.6	0.44	1.4	2.85	4.25
4	3.26	0.4	583	0.53	3.3	1.3	1.37	4.56	0.31	4.87
5	3.00	0.84	None	0.59	3.5	1.3	1.57	4.54	0	4.54
6	3.03	0.74	None	0.56	3.5	1.3	1.58	4.52	0	4.52

treated with various concentrations of nitric acid and with nitric acid-bearing dissolver solutions. The residue, which calculated to be 85 percent uranium tetrafluoride monohydrate, was readily soluble in 1M nitric acid or zirconium fluoride dissolver solution made 1M in nitric acid, as shown in Table IV-2.

Anticipating the possibility of transferring the residue prior to complete dissolution, the particle size range was determined using the method of Andreason(5). Ninety-seven weight percent of the particles in the residue had Stokes' law diameters greater than 4 microns and a median diameter of 10 microns.

It is recognized that the increased exposure to nitric acid will provide corrosion conditions which may prohibit the use of a Monel vessel for dissolving. Corrosion studies are being made to define the limitations of Monel in this respect and to investigate feasible alternate construction materials.

B. Higher Capacity Interim Zirconium Process, H. Schneider, Problem Leader; J. W. Codding, E. E. Erickson, R. F. Murray

During an investigation of zirconium dissolution methods, it was found that an aluminum fluoride-nitric acid slurry was a fairly satisfactory dissolving agent, yielding a stable dissolution product of about 1M in aluminum and 0.5M in zirconium. Such a system suggested the possibility of using existing larger capacity continuous TBP aluminum alloy processing equipment for zirconium processing in view of the relatively noncorrosive nature of the dissolvent, in place of the existing limited capacity hydrofluoric acid process equipment.

Later studies showed that when Zircaloy-2 was substituted for crystal bar zirconium, the aluminum fluoride-nitric acid system gave dissolution rates which were unacceptable for process considerations. This led to the consideration of a modified hydrofluoric acid zirconium dissolution in either the present or a new dissolver, followed by solvent extraction from aluminum nitrate solution in existing higher capacity TBP process columns. Such a processing system might require only minor modifications because of equipment differences. A preliminary flowsheet was developed on this basis. It is considered that dissolution and feed makeup, similar to the present process but with suitable modifications to increase throughput rate, could be carried out in existing hydrofluoric acid process equipment, or in a new continuous dissolver constructed of materials suitable for the hydrofluoric acid system.

Estimations on dissolution capacities led to the conclusion that the simplest means of obtaining increased throughput would be the addition of a second batch dissolver to the present system. A considerable increase over present STR batch dissolver capacity can probably

(5) Herdan, G., Small Particle Statistics, Elsevier Publishing Co., New York, 1953.

Table IV-2

Treatment of Uranium Fluoride Residue from Hydrofluoric Acid Dissolution of Zirconium

Experiment No.	Weight of Residue, Mg	Uranium in Residue, Percent	Reagent	Volume, Ml	Digestion Time, Minutes	Uranium Dissolved, Mg	Observations
I	502		10M HNO_3	25	30		Partial Dissolution
					+30		Small Residue
		62		5	+30	311	~ 5 mg
II	514	--	Diss.Soln. made 1M HNO_3	100	60	---	Complete Dissolution
III	500	--	1M HNO_3	50	60	---	Complete Dissolution
IV	513		0.5M HNO_3	50	60		Partial Dissolution
		59		50	+60	302	Complete Dissolution
V	506	--	0.3M HNO_3	50	60	113	About 35% Dissolution
		61	6M HNO_3	50	+30	197	Complete Dissolution
VI	504	61	10M HNO_3	50	50	308	Complete Dissolution
VII	492	70	Diss.Soln. made 3M HNO_3	100	30	343	Complete Dissolution
VIII	419	--	Diss.Soln. made 5M HNO_3	85	45	---	$ZrF_4 \cdot H_2O$ ppt.

be obtained by increasing the hydrofluoric acid feed rate to the dissolver (provided that the increased off-gas volume is taken into consideration) and preheating the dissolver feed water, thus reducing the cycle time.

Laboratory data on the dissolution of zirconium extrapolated to conditions of continuous dissolution indicate that a single continuous dissolver similar to that provided for aluminum alloy dissolution should give enough capacity. Means would be required for dissolution of tin contained in Zircaloy compositions.

The dissolver solution produced would be essentially identical with that of the present hydrofluoric acid process. Accordingly, the hydrofluoric acid extraction flowsheet was modified somewhat for use in existing aluminum alloy TBP process columns. The most significant modification necessary was the recycle of scrub column raffinate to the first cycle feed, rather than extracting it with fresh organic and discarding it to waste as is done in the present compound scrub column. A decrease in scrub aluminum nitrate concentration from 0.7 to 0.5M avoids possible precipitate formation in the feed after recycle addition, and the feed concentrations have been increased so that the effect of the recycle dilution is to feed a solution to the extraction column of exactly the same composition as currently fed. Another minor change to be considered is due to possible stage efficiency differences between aluminum and zirconium systems; modification in first column volume ratio should be sufficient to overcome any increase in HETS.

Preliminary corrosion tests were made on Type 347 stainless steel, as used for present aluminum nitrate waste storage tanks, immersed in a synthetic waste composed of mixed zirconium fluoride waste and aluminum nitrate waste. A penetration rate of 0.5 mils/year was measured at 50° C. This rate is very similar to the one reported for Type 316 in zirconium fluoride-aluminum nitrate waste and probably acceptable on an interim basis. However, three-year corrosion data on Type 347 stainless steel show a much lower rate in straight aluminum nitrate-nitric acid waste.

C. Electrochemical Aspects of Zirconium Dissolution in Hydrofluoric Acid, C. M. Slansky, Acting Problem Leader; J. R. Aylward

The dissolution of a metal in acid solution is an electrochemical process to which the theory of the mixed potential is applicable. In the dissolution of zirconium in HF solutions, the overall reaction (Equation 1) can be considered as the

$$Zr + 4HF \longrightarrow ZrF_4 + 2H_2 \qquad (1)$$

sum of two electrode reactions (anodic and cathodic), taking place simultaneously at the metal surface (Equations 2 and 3).

$$Zr + 4HF \longrightarrow ZrF_4 + 4H^+ + 4e \qquad (2)$$

$$4H^+ + 4e \longrightarrow 2H_2 \qquad (3)$$

The potential of the dissolving metal will be determined by the overvoltage of both the anodic (Equation 2) and cathodic (Equation 3) reactions; thus the term mixed potential.

In the light of the present day knowledge of electrode kinetics it is reasonable to assume that the cathodic reaction will be mainly activation controlled, but the anodic reaction can be either activation or diffusion controlled. These two cases are treated by the theory of mixed potentials, the object being to express the steady state mixed potential and the reaction rate as a function of the solution composition. This will establish criteria that can be used to distinguish between the activation and diffusion controlled mechanisms. At this time, consideration will be given only to the case where there is no external current applied to the dissolving metal. Under these conditions the anodic (Equation 2) and cathodic (Equation 3) reactions proceed at the same rate ($i_a = i_c$, where i_a and i_c are the anodic and cathodic currents, respectively), and the potential $\mathcal{E}$ of the dissolving metal is called the steady state mixed potential.

Case I: Anodic Reaction is Activation Controlled. The rates (current) of reactions (2) and (3) are related to the steady state mixed potential $\mathcal{E}$ by the following equations.

$$i_a = i_{om}\, e^{\frac{F}{2RT}(\mathcal{E} - \mathcal{E}_m)}, \qquad (4)$$

$$i_c = i_{oH}\, e^{-\frac{F}{2RT}(\mathcal{E} - \mathcal{E}_H)}, \qquad (5)$$

where i_o is the exchange current, $\mathcal{E}_m$ and $\mathcal{E}_H$ the reversible potentials of the anodic and cathodic reactions, respectively (given in Equations 6 and 7).

$$\mathcal{E}_m = \mathcal{E}_m^\circ + \frac{RT}{F} \ln \frac{(a_{ZrF_4})^{1/4}\, a_{H^+}}{a_{HF}} \qquad (6)$$

$$\mathcal{E}_H = \frac{RT}{F} \ln \frac{a_{H^+}}{P_{H_2}^{1/2}} \qquad (7)$$

In the absence of an applied external current $i_a = i_c$, and using Equations 6 and 7, the steady state mixed potential is given by

$$\mathcal{E} = \frac{RT}{F} \ln \frac{i_{oH}}{i_{om}} + \frac{\mathcal{E}_m^\circ}{2} + \frac{RT}{2F} \ln \frac{(a_{ZrF_4})^{1/4}}{a_{HF}} + \frac{RT}{F} \ln \frac{a_{H^+}}{P_{H_2}^{1/2}} \quad (8)$$

Therefore,

$$\frac{\partial \mathcal{E}}{\partial \ln a_{H^+}} = \frac{RT}{F} \quad (9)$$

and

$$\frac{\partial \mathcal{E}}{\partial \ln a_{HF}} = -\frac{RT}{2F}. \quad (10)$$

From Equations 8 and 4 or 5

$$\ln i = \tfrac{1}{2} \ln i_{oH} i_{om} - \frac{F}{4RT} \mathcal{E}_m^\circ - 1/4 \ln \frac{(a_{ZrF_4})^{1/4}}{a_{HF}} \quad (11)$$

Therefore,

$$\frac{\partial \ln i}{\partial \ln a_{HF}} = 1/4 = \frac{\partial \ln \text{Rate}}{\partial \ln a_{HF}}. \quad (12)$$

and

$$\frac{\partial \ln i}{\partial \ln a_{H^+}} = 0 = \frac{\partial \ln \text{Rate}}{\partial \ln a_{H^+}}. \quad (13)$$

Equation 9, 10, 12, and 13 are the criteria for the case where both the anodic and cathodic reactions are activation controlled.

Case II: Anodic Reaction Diffusion Controlled. If it is assumed that the rate determining step of the anodic reaction is the slow diffusion of HF to the metal surface, then it can be shown that the anodic current (rate) is given by

$$i_a = D' C_B \left[1 - \frac{\gamma_B}{\gamma_e} e^{\frac{-F}{RT} (\mathcal{E} - \mathcal{E}_m)} \right] \quad (14)$$

where D' is the diffusion coefficient, C_B the stoichiometric concentration of HF in the bulk of the solution, and γ_B and γ_e are the activity coefficients of HF in the bulk of the solution and at the metal surface, respectively. The equation resulting from equating the anodic and cathodic currents given by Equation 14 and 5, and the substitution of Equation 6 and 7 for $\mathcal{E}_m$ and $\mathcal{E}_H$ can be solved for $\mathcal{E}$ to give

$$\mathcal{E} = \frac{-2RT}{F}\left[\ln \frac{D}{i_{oH}} + \ln C_B\right] + \frac{RT}{F} \ln \frac{a_{H^+}}{P_{H_2}^{1/2}}. \quad (15)$$

It follows that

$$\frac{\partial \mathcal{E}}{\partial \ln C_B} = \frac{-2RT}{F} \quad (16)$$

and

$$\frac{\partial \mathcal{E}}{\partial \ln a_{H^+}} = \frac{RT}{F}. \quad (17)$$

From Equations 15 and 14 or 5 it can be shown that

$$i = D' C_B \quad (18a)$$

or

$$\text{Rate} = \frac{D'}{4F} C_B. \quad (18b)$$

Therefore,

$$\frac{\partial \ln i}{\partial \ln C_B} = 1 = \frac{\ln \text{Rate}}{\ln C_{HF}} \quad (19)$$

and

$$\frac{\partial \ln i}{\partial \ln a_{H^+}} = 0 = \frac{\partial \ln \text{Rate}}{\partial \ln a_{H^+}}. \quad (20)$$

Equations 16, 17, 19, and 20 are the counterparts of 9, 10, 12, and 13 for the case where the anodic reaction is controlled by diffusion. The corresponding equations that are different for the two cases may be used to distinguish between the two mechanisms by comparison with experiment.

The dependence of the rate of a chemical reaction on temperature is also useful in deciding between an activation or diffusion controlled mechanism. From the theory of absolute reaction rates we have

$$\frac{\partial \ln \left(\frac{k}{T}\right)}{\partial \left(1/T\right)} = -\frac{\Delta H^{\ddagger}}{R} \quad (21)$$

where k is the rate constant and $\Delta H^{\ddagger}$ the heat of activation. This equation is true for both activation and diffusion controlled reactions, but for an activation controlled process $\Delta H^{\ddagger}$ is generally greater than 10 K cal/mole. In the case of a diffusion controlled reaction $\Delta H^{\ddagger}$ is related to the viscosity of the solution η by the following equation

$$\eta = A e^{\frac{\Delta H^{\ddagger}}{RT}} \qquad (22)$$

where A is a constant. For aqueous solutions $\Delta H^{\ddagger}$ calculated from Equation 22 has values ranging from 3 to 4 K cal/mole so it is to be expected that a diffusion controlled reaction would have a $\Delta H^{\ddagger}$ in this range.

The following tabulation summarizes the criteria that may be used to distinguish between the activation and diffusion controlled mechanisms. Comparison with experiment is shown where data are available.

Relation	Activation	Experimental	Diffusion
$\frac{\partial E}{\partial \ln C_{HF}}$	$\simeq \frac{-RT}{2F}$	----	$\frac{-2RT}{F}$
$\frac{\partial \ln \text{Rate}}{\partial \ln C_{HF}}$	$\simeq 1/4$	1	1
$\Delta H^{\ddagger}$	>10 K cal	3 to 6 K cal	4 K cal

As can be seen from this table, present experimental evidence indicates that the reaction is diffusion controlled; i.e., the rate determining step is the slow diffusion of HF to the metal surface. To confirm this conclusion, experiments are being planned to test Equation 16

$$\left(\frac{\partial E}{\partial \ln C_{HF}} = -\frac{-2RT}{F} \right).$$

The theoretical investigation will also be extended to include the case where an external current is applied to the dissolving metal.

D. Kinetics of Zirconium Dissolution, C. M. Slansky, Acting Problem Leader; E. M. Vander Wall, E. M. Whitener

1. Effect of the Nitric Acid Concentration on the Dissolution of Zirconium in Mixtures of Nitric and Hydrofluoric Acids

Previous experimental evidence has shown that the initial rate of dissolution of zirconium metal in nitric-hydrofluoric mixtures is dependent on only the undissociated hydrofluoric acid present. Further to confirm these findings, zirconium metal was dissolved at 40 ± 0.5° C in mixtures of 0.5M hydrofluoric acid and various concentrations of nitric acid. The dissolutions were performed using irradiated zirconium coupons, some of which had been previously etched and others not. The data indicate that the nitric acid concentration does not affect the average overall rate, although it may affect the initial rates to a small extent. The initial rates using 2, 5, and possibly 7M nitric acid were apparently greater than at the other concentrations of nitric acid used. However, after a period of 25 minutes these differences disappeared. The data obtained are summarized in Table IV-3. Standard deviations at the 68 percent confidence level were calculated. Much of the deviation may have been caused by variations in the original surface preparation of the samples used.

Table IV-3

Effect of Nitric Acid Concentration on the Dissolution of Zirconium in Dilute hydrofluoric Acid

Initial Hydrofluoric Acid Concentration, 0.5M
Temperature, 40 ± 0.5° C
Volume, 575 ml.
Time of Dissolution, 25 minutes

Initial Nitric Acid Conc., M	Dissolution Rate, Mg/(Cm)^2(Min)	
	Initial	Average
0	5.8 ± 0.3	4.2 ± 0.2
2	6.9 ± 0.3	4.8 ± 0.1
5	6.7 ± 0.1	4.8 ± 0.1
7	6.2 ± 0.9	4.6 ± 0.4
10	5.7 ± 0.6	4.1 ± 0.5
11.3	5.8 ± 0.6	4.5 ± 0.2
13	5.7 ± 0.3	4.3 ± 0.4

2. Dissolution of Zirconium in Nitric-Hydrofluoric Acid at 115° C

The dissolution of zirconium metal in mixtures of nitric and hydrofluoric acids at 115° C was performed in a glass apparatus. The rate of dissolution was followed by periodically removing the coupon from the solution for measurement and replacing it immediately with another coupon. This procedure reduced the corrosion of the glassware by the hydrofluoric acid. The nitric acid concentration was maintained at 13M while the hydrofluoric acid concentration was varied up to 0.75M. A plot of the initial rate of dissolution of zirconium versus the initial hydrofluoric acid concentration is given in Figure IV-1. At concentrations above 0.25M hydrofluoric acid, the attack on the glassware by the hydrofluoric acid became appreciable. This would account for the deviation from linearity of the points at 0.5 and 0.75M hydrofluoric acid. The rate constant for the dissolution based on 0.25M hydrofluoric acid was found to be 66 mg/(sq.cm)(min)(mole HF/liter). The resulting solutions which had a fluoride-zirconium ratio of two or somewhat less were stable and clear.

A plot of this rate constant along with the rate constants at 40-60° C gives an activation energy of approximately 6 kcal-mole^{-1} for the dissolution as shown in Figure IV-2. An activation energy of this order indicates that the reaction is probably diffusion controlled.

In order to determine whether or not the assumption that the actual area of the zirconium coupons is proportional to the apparent area was legitimate, the initial rate of dissolution was determined using two zirconium coupons instead of one. This effectively doubled the surface area which was subject to dissolution. The average initial rate constant in the case where the area was doubled was 64.2 $\pm$ 2.9 as compared to 71.2 in the case where the single coupon was used.

3. Dissolution of Zircaloy-2 in Mixtures of Nitric and Hydrofluoric Acids at 115° C

Coupons cut from a plate of Zircaloy-2 were dissolved at 115° C in mixtures of 13M nitric acid and various concentrations of hydrofluoric acid. The glass system used for the zirconium dissolution was again employed in the dissolution of Zircaloy-2 and the same method was used to follow the course of the dissolution. The data obtained from these experiments are given in Figure IV-3.

In this case the deviation from a linear relationship of initial dissolution rate and initial hydrofluoric acid concentration is less than in the case of zirconium. The rate of attack on the glassware in these dissolutions appeared to be comparable to that in the dissolutions using pure zirconium. The rate constant evaluated from the slope of the line in Figure IV-2 for the initial rate was 63 which is essentially the same as the value of 66 obtained for pure zirconium. The resulting solutions from the dissolution of Zircaloy-2, in which the fluoride-zirconium ratio

FIGURE IV-1

EFFECT OF HF CONCENTRATION ON DISSOLUTION RATE OF ZIRCONIUM AT 115°C

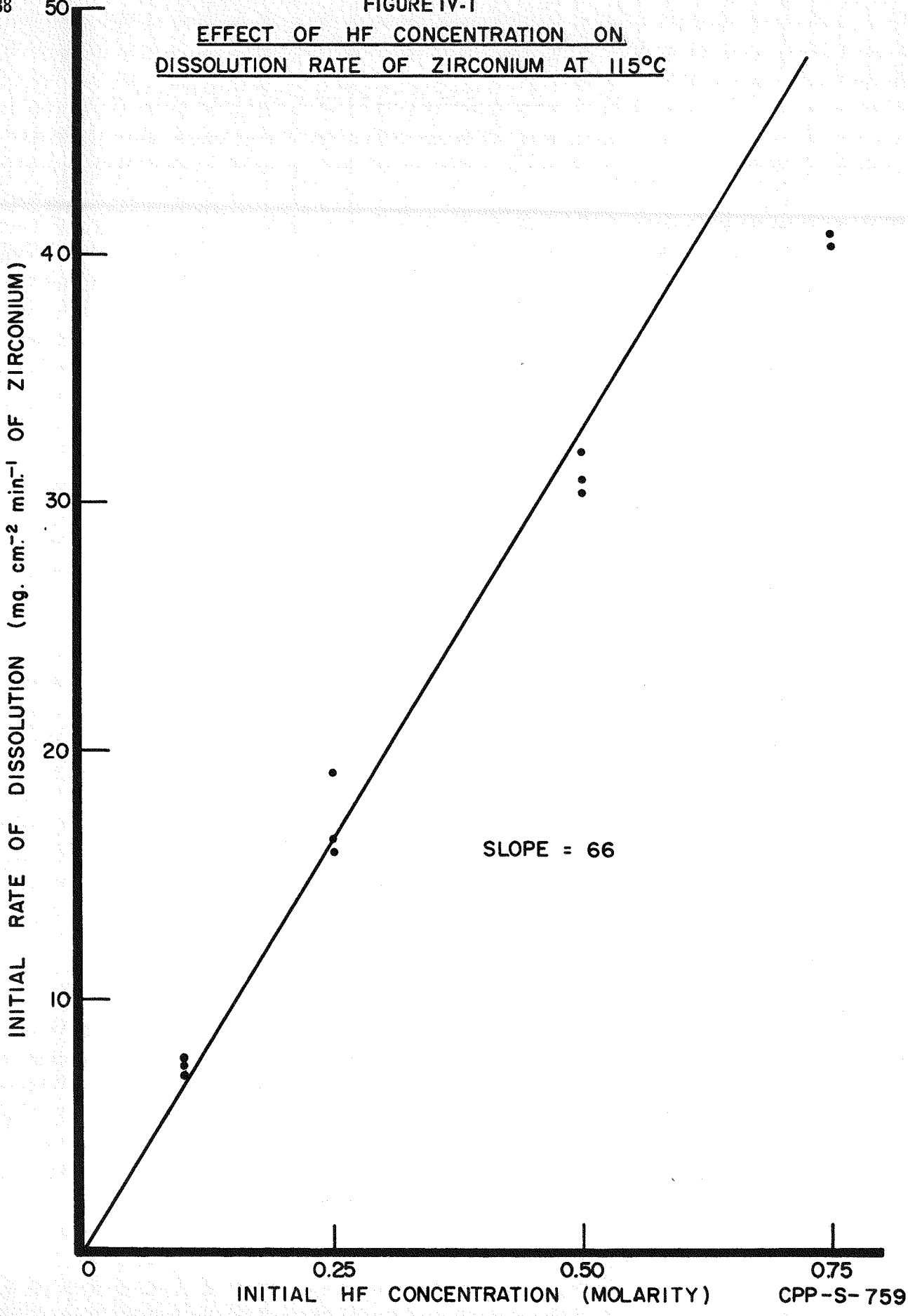

FIGURE IV-2

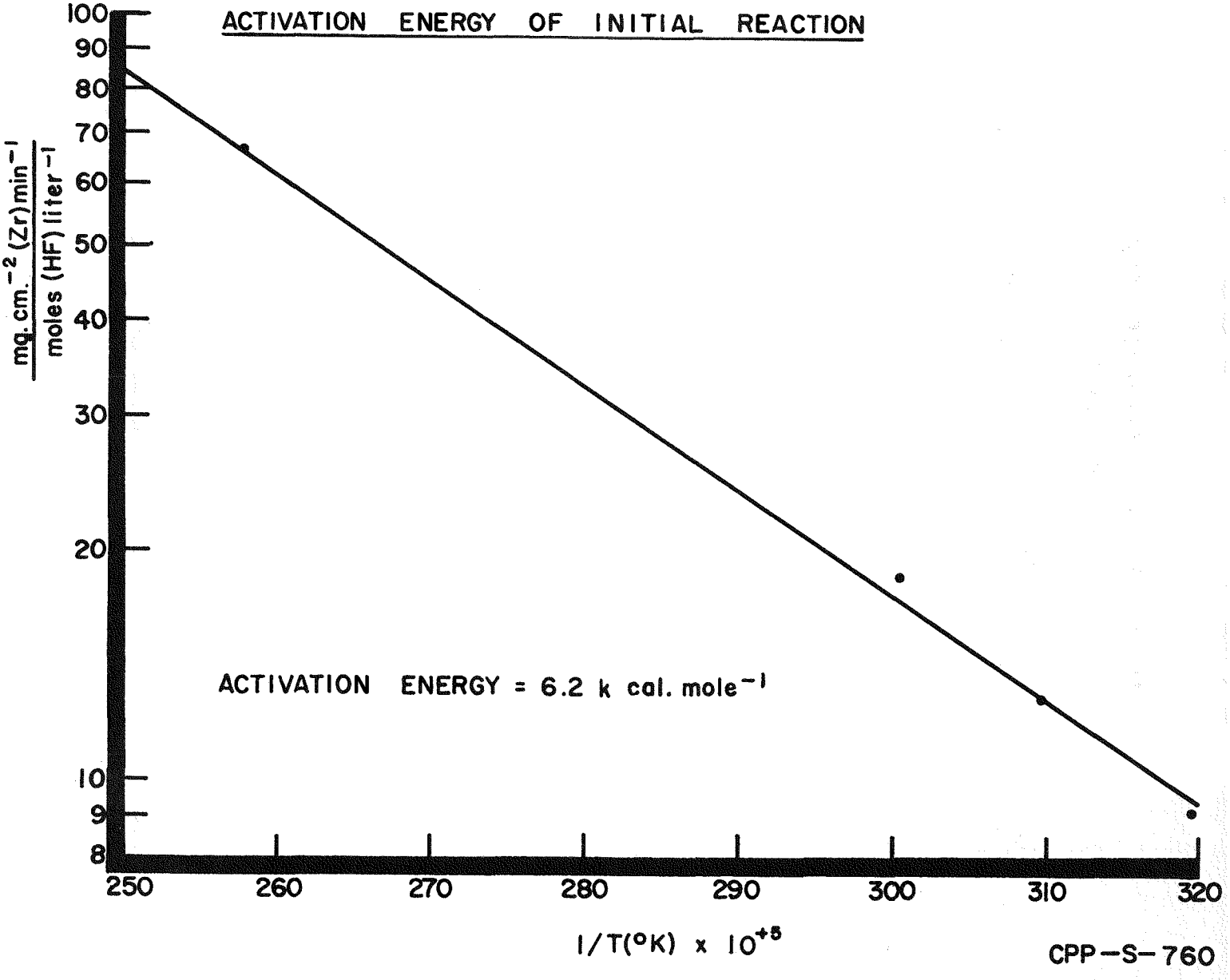
ACTIVATION ENERGY OF INITIAL REACTION
mg. cm.$^{-2}$ (Zr) min^{-1} / moles (HF) liter^{-1}
100
90
80
70
60
50
40
30
20
10
9
8
ACTIVATION ENERGY = 6.2 k cal. mole^{-1}
250
260
270
280
290
300
310
320
1/T(°K) x 10^{+5}
CPP-S-760

FIGURE IV-3
DISSOLUTION OF ZIRCALOY-2 IN NITRIC-HYDROFLUORIC ACID MIXTURES

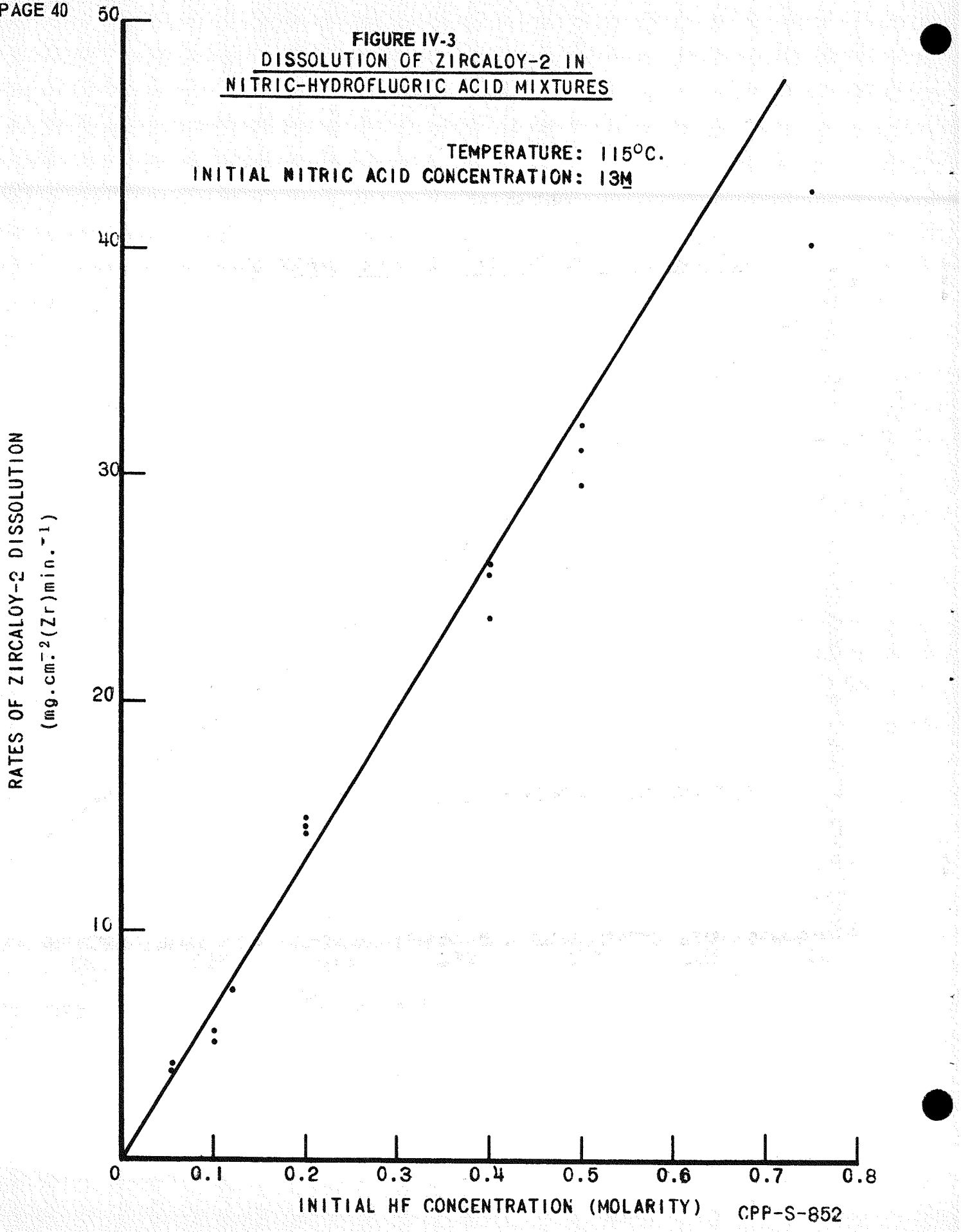

was 2 or less, all contained a precipitate which contained both tin and zirconium. The presence of some zirconium in the precipitate was surprising in that no precipitate of zirconium appeared in the solutions resulting from the dissolution of pure zirconium. Identification of all the components in the precipitates has not as yet been completed. Preliminary results indicate that all the tin present in the Zircaloy-2 precipitates out of solution during dissolution in concentrated nitric acid.

4. Mixtures of Various Fluorides and 13M Nitric Acid for the Dissolution of Zirconium

Dissolution of zirconium metal was performed in mixtures containing 13M nitric acid and calcium, aluminum, or zirconium fluorides.

Mixtures containing 200 ml of 13M nitric acid and approximately 25 grams of aluminum fluoride (61 percent AlF_3) were used to dissolve zirconium metal. The dissolutions were performed in a glass apparatus at 115° C. The average rate for the first five minutes of dissolution was 10.5 ± 0.8 mg/(sq.cm)(minute); the average rate for the first thirty minutes of dissolution was 8.3 ± 0.3 mg/(sq.cm)(minute). The solution clarified when the total fluoride-to-zirconium ratio was 2.8 - 3.0. The average rate of dissolution until the solution clarified was 4.7 ± 0.14 mg/(sq.cm)(minute) and the instantaneous rate at the time of clarification was 2.6 ± 0.14 mg/(sq.cm)(minute).

The initial rate obtained with 13M nitric acid and excess aluminum fluoride at 115° C corresponds to the rate obtained with approximately an initial concentration of 0.16M hydrofluoric acid and 13M nitric acid.

Mixtures containing 200 ml of 13M nitric acid and various amounts of calcium fluoride were used to dissolve zirconium metal. These dissolutions were also performed in a glass apparatus at 115° C. The initial rate for the first three minutes was approximately 21 mg/(sq.cm)(minute). This rate fell off rapidly to a constant value of 8-9 mg/(sq.cm)(minute) where it remained until the fluoride-to-zirconium ratio reached 5. At this point the rate began to decrease so that when the solution clarified at a fluoride-to-zirconium ratio of approximately 2, the rate was of the order of 4 mg/(sq.cm)(minute).

It is possible that the sharp decrease in the rate initially is due to the formation of a calcium fluozirconate complex which decreases the available hydrofluoric acid concentration. The initial rate is comparable to that obtained with 0.3M hydrofluoric acid and 13M nitric acid, while the rate of 8-9 mg/(sq.cm)(minute) is comparable to that obtained for 0.13M hydrofluoric acid and 13M nitric acid.

Mixtures containing 200 ml of 13M nitric acid and various amounts of zirconium tetrafluoride monohydrate were also used for

dissolution of zirconium metal. A mixture containing 25 grams of the zirconium tetrafluoride gave an initial rate of 13.8 mg/(sq.cm)(minute) and 12.6 mg/(sq.cm)(minute) as the average rate for the first thirty minutes. The initial rate corresponds to the rate obtained with 0.2M hydrofluoric acid and 13M nitric acid. Because of the several complexes which zirconium can form with fluoride, there is a general decrease in the rate of dissolution when these mixtures are used. The mixture of zirconium tetrafluoride and nitric acid did not clarify during the dissolution as occurred with both calcium and aluminum fluorides.

E. Solid Phase Studies in Zirconium-Nitric Acid-Hydrofluoric Acid Systems, C. M. Slansky, Acting Group Leader; A. G. Chapman

Study of the equilibrium relationships in the zirconium fluoride-nitric acid system was continued in an effort to develop a solid phase diagram for this system. At least three solid zirconium fluoride compounds have been found to exist in equilibrium with nitric acid of concentrations from 1 to 16M and at temperatures from 0 to 80° C. The composition and equilibrium ranges in nitric acid are approximately as follows: (1) zirconium tetrafluoride monohydrate, $ZrF_4 \cdot H_2O$, a relatively dense crystalline solid, is the stable solid phase in equilibrium with nitric acid more concentrated than 8M and at all temperatures from 0 to 80° C and in nitric acid concentration higher than about 6M at temperatures above 50-55° C; (2) zirconium tetrafluoride trihydrate, $ZrF_4 \cdot 3H_2O$, a relatively dense crystalline solid, is the equilibrium phase in nitric acid below about 6M and at temperatures less than about 55° C; and (3) a less dense crystalline solid having an unidentified X-ray diffraction pattern and having a chemical composition of approximately 3 moles of fluoride to 1 mole of zirconium, is found in nitric acid concentrations less than approximately 4M and at temperatures above about 50 - 55° C. Nitrate ions are not detected in these solid phases, which indicates there is very little tendency for nitrate to exchange for fluoride in zirconium tetrafluoride in nitric acid of wide concentration ranges.

Thermal degradation of the solid phases in both air and water vapor at temperatures from 100 to 310° C did not produce solids having the same X-ray diffraction pattern as those taken from the dilute nitric acid system at elevated temperatures. Further study of these solids is being made.

F. Zirconium Extraction Studies, K. L. Rohde, Problem Leader; R. L. Hickok

The extraction of zirconium by tributyl phosphate (TBP) from systems of nitric acid and mixed nitric and hydrofluoric acids was further studied. Application of the technique of exhaustive equilibration to a system in

which the zirconium and fluoride concentrations were in the range of 0.01 to 0.1M made possible more critical examination of the zirconium species extracted and of the extraction equilibria involved. It has been found that the presence of fluoride in amounts which result in a mole ratio of fluoride to zirconium less than about 1.5 to 1 in the equilibrium aqueous phase tends to increase slightly the distribution of zirconium into TBP. This effect is greater at low concentrations of nitric acid and decreases to zero in solutions somewhat above 6M in nitric acid. The mole ratio of extracted fluoride to extracted zirconium increases with increasing aqueous fluoride concentration but does not reach a value of 2 in systems from which zirconium extraction is chemically measurable.

The objectives of this work were to study the mechanism, or mechanisms, by which zirconium is extracted by TBP from nitric acid systems with and without fluoride. The determination of equilibrium constants involved in the extraction of the various species was attempted. The method employed in this study was to examine the effects of nitric acid and total aqueous fluoride concentrations on the distribution of zirconium into TBP using the techniques of exhaustive equilibration and radiochemical analysis of zirconium. Using these techniques the following systems were studied: (1) 0.0115M Zr - variable HNO_3 - 1.0M TBP; (2) 0.0117M Zr - variable HNO_3 - 0.30M TBP; (3) 0.0115M Zr - 0.0151M HF - variable HNO_3 - 1.0M TBP; (4) 0.115M Zr - 0.151M HF - variable HNO_3 - 1.0M TBP; (5) 0.115M Zr - 6.33M HNO_3 - variable HF - 1.0M TBP. In addition, six single pass extractions were conducted in which zirconium was extracted into 1M TBP from solutions having initial compositions 0.56M Zr, 7M HNO_3 and variable HF concentrations. This experiment was designed to determine the mole ratio of extracted fluoride to extracted zirconium.

In all of these experiments the TBP was diluted with n-dodecane except for a few of the extractions in series (1) and (2), in which n-heptane was used to increase the solubility of the zirconium-TBP complex in the organic phase. The preparation of the aqueous zirconium solutions and the purification of TBP and the organic diluents have been previously described (IDO-14422, IDO-14430).

The exhaustive equilibrations were carried out by shaking 10 ml of the extractant solution with successive equal volume portions of a given zirconium solution, labeled with freshly separated zirconium-95 tracer. The equilibrations were continued until the gamma counting rate, as determined in a well-type scintillation counter, of 2 ml portions of successive raffinates agreed within about one percent with a sample of the original stock solution. Toward the end of an experiment 2 ml portions of the extract phase were also counted following successive extractions confirming the approach to equilibrium. Where solubility difficulties prevented attainment of equilibrium both phases were counted after each of several equilibrations prior to the appearance of the second organic phase. The distribution coefficients obtained in this way do not represent equilibrium between the aqueous stock solution,

of selected composition, and a loaded TBP phase; but it is likely that equilibrium with respect to nitric acid distribution was achieved, thus allowing reasonably accurate calculation of the free TBP concentration.

From data for the equilibrium composition of the aqueous solutions and the experimentally determined distribution coefficients, the free TBP concentrations were determined. The concentration of the uncombined TBP was calculated by the method of Donadien[6] as follows:

$$(TBP)_f = \frac{(TBP)_t - n\,(Mo)}{1 + K_H(H^+)(NO_3^-)}$$

where

$(TBP)_t$ = total TBP concentration

n = number of TBP molecules complexed per metal atom

= 2 for zirconium

(Mo) = concentration of metal in the organic phase

K_H = equilibrium constant for the extraction of nitric acid into TBP

= 0.20

The concentration of hydrogen and nitrate ions were calculated from the nitric acid concentration and the degree of dissociation of nitric acid, but was somewhat modified for solutions in which the contribution of nitrate ion from the zirconium nitrate was significant.

Typical results of the exhaustive equilibrium extraction experiments are given in Table IV-4, data for single equilibrations are contained in Table IV-5, and the data are summarized in Figures IV-4 to IV-6.

Previous experiments have shown that the zirconium-TBP complex formed in the extraction has two TBP molecules complexed per zirconium atom. This is in agreement with the conclusion reached by McKay[7] and is analogous to the TBP extraction of thorium nitrate. To investigate accurately the effects of nitric acid or aqueous fluoride on the distribution it is necessary to calculate the equilibrium concentration of uncombined TBP and to normalize the distribution coefficients to a selected free TBP concentration. With the data in this form it is then possible to develop equilibrium equations to which the data can be applied. This was done as follows:

(6) Donadien, L. J., Thesis, M. I. T., 1956

(7) KcKay, H. A. C., et. al., The Extraction of Zirconium by Tributyl Phosphate, AERE-C/R-923, 10F1, (Confidential)

Table IV-4

Extraction of Zirconium from Nitrate and Fluoride Systems by Tributyl Phosphate

Temperature: 23° C
Typical Data Obtained by Exhaustive Equilibration

Equilibrium Aqueous Composition			Solvent, Moles TBP per Liter Dodecane	Zirconium Distribution Ratio, O/A	Free TBP in Solvent (TBP_f), M	Normalized Zirconium Distribution $E_A^O/(TBP_f)^2$
Nitric Acid, M	Zirconium M	Fluoride M				
0.504	0.0115	0.0	1.0	0.0049	0.953	0.0054
1.48	0.0115	0.0	1.0	0.026	0.707	0.024
2.45	0.0115	0.0	1.0	0.068	0.490	0.28
3.43	0.0115	0.0	1.0	0.16	0.354	1.28
4.40	0.0115	0.0	1.0	0.375	0.273	5.0
5.38	0.0115	0.0	1.0	0.813	0.228	15.5
6.31	0.0115	0.0	1.0	1.61	0.209	36.9
6.79	0.0115	0.0	1.0	2.20	0.204	52.6
0.01	0.0117	0.0	0.3	~0.0	0.3	~0.0
0.28	0.0117	0.0	0.3	0.0005	0.295	0.006
2.48	0.0117	0.0	0.3	0.0090	0.145	0.43
6.93	0.034	0.0	0.3	0.12	0.59	34.
0.50	0.0115	0.0154	1.0	0.0154	0.954	0.0121
0.99	0.0115	0.0154	1.0	0.03	0.845	0.044
1.95	0.0115	0.0154	1.0	0.074	0.596	0.21
2.44	0.0115	0.0154	1.0	0.108	0.494	0.44
3.40	0.0115	0.0154	1.0	0.226	0.358	1.76
4.40	0.0115	0.0154	1.0	0.44	0.271	6.01
5.38	0.0115	0.0154	1.0	0.77	0.224	15.2
6.35	0.0115	0.0154	1.0	1.25	0.204	30.1
6.84	0.0115	0.0154	1.0	1.53	0.198	39.0
9.03	<0.01	<0.0154	1.0	4.5	0.193	121
1.26	0.115	0.155	1.0	0.0287	0.958	0.0312
3.26	0.115	0.155	1.0	0.190	0.338	1.67
4.26	0.115	0.155	1.0	0.314	0.247	5.15
5.26	0.115	0.151	1.0	0.751	0.151	32.9
6.33	0.115	0.0	1.0	0.78	0.169	27.3
6.33	0.115	0.160	1.0	0.817	0.167	29.3
6.33	0.115	0.266	1.0	0.201	0.197	5.18
6.33	0.115	0.372	1.0	0.039	0.204	0.94
6.33	0.115	0.509	1.0	0.0075	0.206	0.18

Table IV-5

Zirconium Extraction by Tributyl Phosphate

Temperature: 23° C
Initial aqueous composition: 0.557M Zr, 7.33M nitrate
Solvent: 1.0M TBP in dodecane
Method: Single equilibrations, equal phase volumes

Initial Aqueous Fluoride Conc., M	Initial Aqueous F/Zr Mole Ratio	Raffinate Composition				Molar Decrease in Aqueous Phase Conc., of		Moles Zr Extracted per Mole Remaining	Mole Ratio of Fluoride to Zirconium Extracted
		Zirconium M	Fluoride M	Nitrate M	F/Zr Mole Ratio	Zirconium	Fluoride		
0	0	0.435	0	6.39	0	0.122	0	0.28	0
0.25	0.45	0.391	0.196	6.35	0.50	0.166	0.05	0.43	0.30
0.50	0.90	0.365	0.368	6.50	1.0	0.192	0.13	0.53	0.68
0.75	1.4	0.378	0.576	6.53	1.52	0.179	0.13	0.47	0.73
1.00	1.80	0.440	0.819	6.53	1.86	0.117	0.18	0.27	1.6
1.25	2.24	0.494	1.14	6.57	2.31	0.063	0.11	0.13	1.8
1.50	2.69	0.549	1.44	6.55	2.62	0.010	0.06	0.02	6

FIGURE IV-4

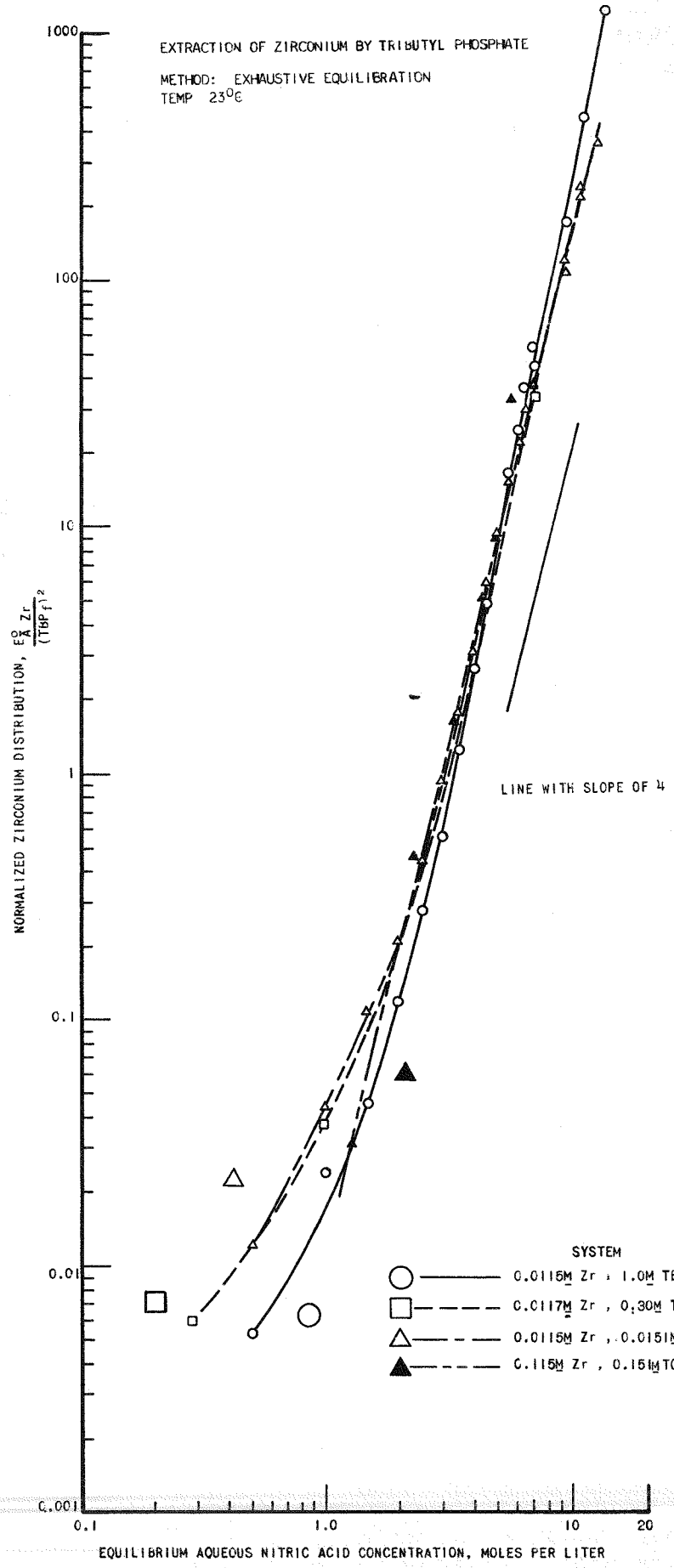

FIGURE IV-5 IDO-14443
PAGE 47

ZIRCONIUM EXTRACTION BY TRIBUTYL PHOSPHATE

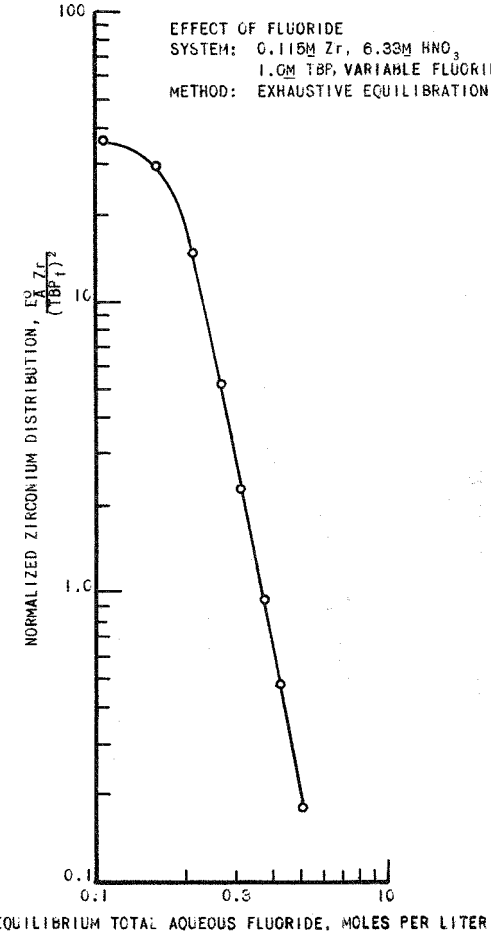

FIGURE IV-6

ZIRCONIUM EXTRACTION BY TRIBUTYL PHOSPHATE

EFFECT OF FLUORIDE

SYSTEM: INITIAL CONCENTRATIONS
0.56M Zr, 7M HNO_3, 1.0M TBP
VARIABLE TOTAL AQUEOUS FLUORIDE

METHOD: SINGLE EQUILIBRATION

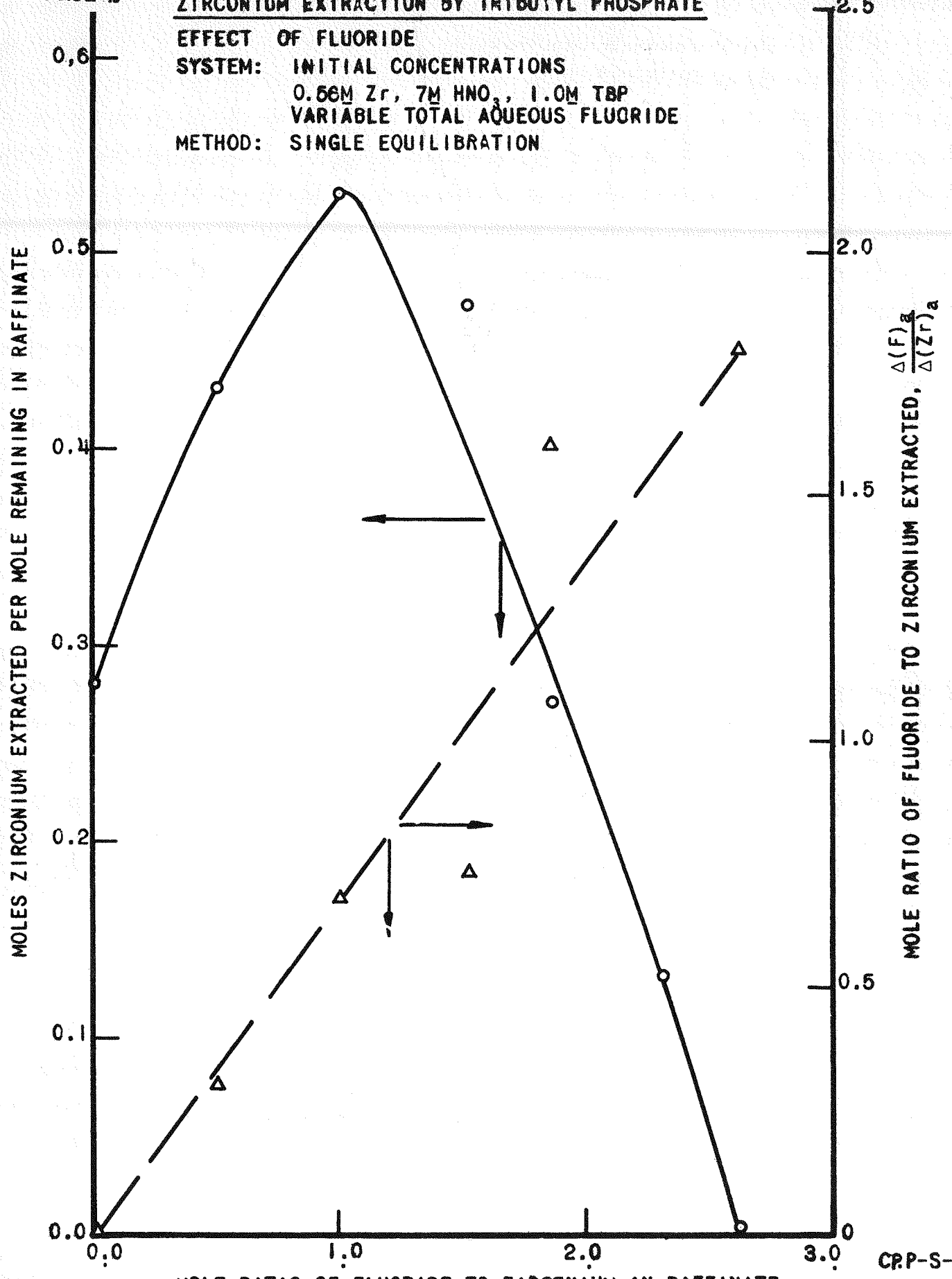

CRP-S-854

The equilibrium constants for the formation of the first three ZrF_4^{+4-n} complexes have been determined by Connick and McVey(8).

$$Zr^{+4} + HF \underline{\underline{k_1}} ZrF^{+3} + H^+, \quad k_1 = 6.3 \times 10^5 \tag{22}$$

$$ZrF^{+3} + HF \underline{\underline{k_2}} ZrF_2^{+2} + H^+ \text{ x}, \quad k_2 = 2.10 \times 10^4 \tag{23}$$

$$ZrF_2^{+2} + HF \underline{\underline{k_3}} ZrF_3^{+} + H^+, \quad k_3 = 6.7 \times 10^2 \tag{24}$$

McVey(9) has also determined the equilibrium constants for the formation of the first two nitrate complexes.

$$Zr^{+4} + NO_3^- \underline{\underline{k_1'}} Zr\ NO_3^{+3} \quad k_1' = 0.503 \tag{25}$$

$$Zr^{+4} + 2NO_3^- \underline{\underline{k_2'}} Zr(NO_3)_2^{+2} \quad k_2 = 0.077 \tag{26}$$

The extraction of the three possible species may be described as follows:

$$Zr_a^{+4} + 4\ NO_{3\ a}^- + 2\ TBP_o \underline{\underline{k_{e1}}} Zr\ (NO_3)_4 \cdot 2TBP_o \tag{27}$$

$$k_{e1} = \frac{(Zr\ (NO_3)_4 \cdot 2TBP)}{(Zr^{+4})(NO_3^-)^4(TBP)^2}$$

$$Zr_a^{+4} + HF_a + 3\ NO_{3a}^- + 2\ TBP_o \underline{\underline{k_{e2}}} ZrF\ (NO_3)_3 \cdot 2TBP_o + H^+ \tag{28}$$

$$K_{e2} = \frac{(Zr\ F\ (NO_3)_3 \cdot 2TBP)_o(H^+)}{(Zr^{+4})_a\ (HF)_a\ (NO_3^-)_a^3\ (TBP)_f^2}$$

$$Zr^{+4} + 2\ HF_a + 2\ NO_{3a}^- + 2\ TBP_o \underline{\underline{k_{e,3}}} ZrF_2\ (NO_3)_2 \cdot 2TBP + 2H^+ \tag{29}$$

$$K_{e\,3} = \frac{(ZrF_2\ (NO_3)_2 \cdot 2TBP)}{(Zr^{+4})_a\ (HF)_a^2\ (NO_3^-)_a^2\ (TBP)_f^2}$$

The measured distribution coefficient, E_A^o is given by

$$E_A^o = \frac{\text{Total zirconium concentration in the organic phase}}{\text{Aqueous zirconium concentration}} \tag{30}$$

$$E_A^o = \frac{(Zr\ (NO_3)_4 \cdot 2TBP) + (ZrF\ (NO_3)_3 \cdot 2TBP) + (ZrF_2\ (NO_3)_2 \cdot 2TBP)}{(Zr^{+4}) + (ZrF^{+3}) + (ZrF_2^{+2}) + ZrF_2^{+}) + Zr\ (NO_3)^{+3}) + (Zr(NO_3)_2^{+2})} \tag{31}$$

(8) Connick, R. E. and McVey, W. H., The Aqueous Chemistry of Zirconium, AECD-2272, March 1, 1948. (Declassified)

(9) McVey, W. H., Zirconium Chemistry, the Nitrate and Thenotl Trifluoroacetone Complexes and the Hydrolytic Species, HW-21487, June 29, 1951, (Unclassified)

The terms in the denominator are assumed to include all zirconium species present in significant concentration.

Combination of Equations 22, 29, and 31 gives

$$\frac{E^o_a}{(TBP)^2_f} = \frac{k_{e1}\,(NO_3^-)^4 + k_{e2}\,(NO_3)^3\,\frac{(HF)}{(H^+)} + k_{e3}\,(NO_3)^2\,\frac{(HF)^2}{(H^+)^2}}{1 + k_1\,\frac{(HF)}{(H^+)} + k_1k_2\,\frac{(HF)^2}{(H^+)^2} + k_1k_2k_3\,\frac{(HF)}{(H^+)^3} + k_1\,(NO_3^-) + k_2'\,(NO_3^-)^2} \quad (32)$$

Equation 32 was applied to the data for 6.33M nitric acid with varying fluoride in an attempt to obtain values for k_{e1}, k_{e2}, and k_{e3}. It was necessary to calculate the concentration of HF in each solution from the equilibrium constants of formation of the zirconium fluoride complexes and the total fluoride and hydrogen ion concentration. Satisfactory evaluation of the equilibrium extraction constants has not yet been completed but preliminary values of about 0.3 and 10^{-5} have been obtained for k_{e1} and k_{e2}, respectively. Further study of the data and application of activity coefficients as they are available or can be estimated should result in more accurate values for the constants.

G. Zirconium Fuel Continuous Dissolving Pilot Plant, J. A. Buckham, Problem Leader; A. F. Boeglin, M. D. Martin

Detailed design and equipment ordering for a pilot plant facility to test various aqueous headend processing schemes for zirconium-bearing fuels has been completed. This pilot plant, constructed essentially from Carpenter-20 alloy, is expected to be ready for operation in four or five months. The principal piece of equipment in this pilot plant is a two-inch diameter continuous dissolver; other equipment includes dissolver feed makeup and dissolver feeding tanks, heat exchangers, dissolver run-down tanks, off-gas disposal system including a caustic scrubber, and suitable instrumentation. It is intended to use this pilot plant both for testing processes for low zirconium content (up to twenty percent zirconium) fuels and for high zirconium content (over ninety percent zirconium) fuels. Low zirconium content fuel flowsheets to be tested all utilize fairly concentrated nitric acid with appropriate minor amounts of hydrofluoric acid and aluminum nitrate as a dissolving reagent. The pilot plant can utilize such flowsheets at rates up to six liters per hour. A wide variety of flowsheets will be tested for the high zirconium content fuels; flow rates up to sixty liters per hour will be used with such dissolving reagents as about 8M hydrofluoric acid containing up to 1M nitric acid and up to nearly two molar aluminum nitrate. Other flowsheets envisioned utilize considerable quantities of fluoride ion in various forms.

V. DEVELOPMENT OF PLANT PROCESS MONITORING INSTRUMENTATION

A. Recycled Raffinate Uranium Monitor, H. Schneider, Problem Leader; R. B. Kimball, R. G. Bearden, L. G. Schwieger

A monitor has been developed for indicating buildup of uranium in the second and third extraction cycle raffinates. In order that these raffinates may be continuously recycled as scrub to the first extraction cycle, it is necessary to monitor the uranium content of these streams continuously as a criticality safeguard. A laboratory model of a photometer developed for this purpose was previously described (IDO-14422). Design and fabrication of two plant models of this instrument have been completed. These will be installed in the plant as soon as brief laboratory tests are completed.

The plant instruments are basically similar to the laboratory model; that is, the same type of light source, optical filters, (Corning No. 5113 and Farrand No. 530) and photovoltaic cell light detector (GE-PV10) have been used. The sample cell and filter change mechanism were redesigned for plant application but are basically similar to the laboratory model. Only minor changes in the measuring system were made. Because of the specific application intended for the instruments, namely that of criticality safeguard, it was necessary to insure that instrument failure could not go undetected for a period of more than ten minutes. For this purpose an instrument failure alarm system was designed and built into the plant model.

The basic element of the alarm system is a relay which is normally energized through a series of cam-operated SPDT micro switches which are connected to form an "AND" logic circuit. If the relay becomes de-energized, a battery operated alarm is energized. This yields direct protection against power failure and relay armature failure.

In addition to the reference cycle and analysis cycle previously described, a third check cycle has been provided in the plant models as a part of the failure alarm system. During the check cycle which immediately follows the reference cycle the output of the servo memory unit is compared with the photovoltaic cell output with the reference filter in place and the error signal is applied to the recorder. Any component malfunction in the memory unit or recorder will not yield the zero reading which is normally observed. A microswitch on the recorder drive senses the position of the pen. A second microswitch on the cycle programmer samples the condition of the recorder position sensing switch. If both switches are closed the alarm relay remains energized. If either switch is open, the relay is de-energized and the failure alarm is sounded. The latter will occur if the recorder reading is any value except zero. By using the dual switch system, switch failure can also be detected. Light source failure or an empty sample cell can be detected in this manner by limiting the output from the memory unit so that balance cannot be obtained for either event

and an error signal will result. As the instrument proceeds to the analysis cycle both switches are moved to the open position and the alarm relay remains energized through this alternate path. The recorder switch is opened because the output of the photovoltaic cell with the analysis filter in place is less than that with the reference filter. Thus, when the filter change is made, an error signal is produced which causes the recorder to move from the zero position. Filter thicknesses were adjusted to produce the unequal signals. If the filter change does not take place, the recorder will remain zeroed holding the recorder switch closed while the programmer switch opens, thereby de-energizing the alarm relay. The same situation would occur if the photovoltaic cell should become desensitized.

Since the programmer is the heart of the control system, its failure must also be detected. For this purpose two separate programmers operating on the same time bases are used. One of the cam-operated switches on each unit is used for tracking the other. The cams on each unit hold the switches open for 180 degrees and closed for 180 degrees. These are set in phase so that both switches are either closed or open. If the units get out of phase one switch will open while the other is closed and the alarm relay will be de-energized. Thus, if either programmer fails or if the switches fail the alarm is sounded. The simultaneous failure of both programmers or switches would go undetected but this is an extremely low probability.

The cell flow system has been designed so that failure of the sample circulating system will result in cell drainage. As previously mentioned, an empty cell will be detected by the alarm system. It is possible, however, that the cell drain line could become plugged and remain undetected so that cell drainage would not occur. To reduce this probability to a minimum, a thermoelectric flow alarm will be included in the cell drainage line. The flowmeter is designed so that any high probability component failure will cause the system to alarm. Low probability failures are not guarded against since this is a secondary alarm.

VI. TESTING AND DEVELOPMENT OF PROCESS EQUIPMENT

G. W. Walpert, Problem Leader; F. A. Graf

A. Pump Development

1. Chempumps Under Life Tests

A pair of Model SF-3/4 horsepower Type 316 stainless steel Chempumps were under test during the past three months. One pump is equipped with Type GBF reactor grade graphite bearings, while the other has the vendor's Graphitar No. 14 bearings.

Bearing wear on the pump equipped with the reactor grade graphite is becoming difficult to ascertain, since the inside diameter of the bearing is out-of-round and bits of graphite dust are deposited on the graphite surface, giving it a false diameter and wear rate. The effects of these factors can be seen in the wear measurements reported.

Comparison of bearing wear with the pump with the Graphitar No. 14 bearings cannot very well be made. The latter pump had a new armature can installed at the 1000-hour check. It was also rebalanced and put into service again at that time. At the 2000-hour check it was noticed that the journal area of the shaft was very badly galled so that the front bearing wore excessively. The damage to the shaft presumably occurred at the time the pump was balanced. For these reasons it was decided to discontinue the tests on the damaged unit and redesign the bearings for maximum area. The modified pump parts were built and are ready for balancing.

Average wear was as follows:

For Pump Equipped With	Bearing Position	Average Cumulative Diametral Wear, Inches, After 1000 Hrs.	2000 Hrs.	3000 Hrs.	4000 Hrs.
Graphite No. 14 Bearings	Front	0.00015	0.00073	Test Discontinued	
	Rear	0.00020	0.00103		
GBF, Reactor Graphite Bearings	Front	0.00026	0.00053	0.00103	0.0015
	Rear	0.00020	0.00040	0.00083	0.0010

It is now planned to run to about 6000 hours on the pump with GBF reactor grade graphite bearings and then install porous alumina bearings for evaluation. This change will allow a comparison between graphite and alumina. With the other pump, a comparison between the two bearing designs can be had so that it is possible to have a rough cross-comparison between the two pumps.

The two test pumps thus far have not had as high wear rates as previously experienced for some Chempumps. This is probably due to the fact that the fluid temperature is near 60° F and the pumping rate of 2.2 gpm allows adequate cooling of the bearings as compared to higher fluid temperatures and lower flow rates in other service. Another favorable factor is the cleanliness of the fluid. Commercially available reagents usually contain some grit or dirt which score the soft bearings. Future plans call for evaluation of porous alumina and pyroceram glass as bearing materials, if available.

Chempumps as received will hold up about a year under continuous duty with aluminum nitrate-nitric acid solution, if the impeller is securely fastened, the fluid temperature within the pump is low, and the stream is clear. The better bearing materials that will be tested in the future may yield a pump life of several years with clear solutions, and longer than previously experienced with solid-bearing streams.

2. Large Pilot Plant Calciner Feed Pump

A Model SF-3/4 horsepower Carpenter-20 Chempump which previously had failed was put back into operation pumping a fine slurry (5 micron or less) of aluminum oxide. The shaft journals were flame-sprayed with alumina and the bearings had inserts which were also flame-plated. Wear tests will be made.

B. Plastic Coatings to Prevent Tubing Air Leaks

Various types of plastic coatings were studied and tested in order to find a suitable coating that would seal aluminum tubing connectors. The Furane Plastics, Incorporated, Epibond 126 with hardener 9812 was chosen as most suitable after several successful tests.

VII. DEVELOPMENT OF FLUID BED CALCINATION PROCESS FOR ALUMINUM NITRATE WASTES

A process is being developed for the conversion of highly radioactive aluminum nitrate processing waste solutions to alumina for storage in solid form. Decomposition is effected in a heated fluidized bed of alumina and radioactive contamination must be removed from the gases generated. Studies were conducted on adsorption of ruthenium from off-gas by silica gel and stainless steel, venturi scrubbing and electrostatic precipitation of particles contained in off-gases, and heating the bed by direct-fired tubes and by circulating hot liquid metal. Measurements of thermal conductivity of alumina at high temperatures were continued, and attrition of alumina when moved in storage was estimated. Removal of fission products by dilute acid leaching was investigated. The development of a suitable overall process design was carried along.

A. Removal of Ruthenium from Simulated Raw Calciner Off-Gas,

K. L. Rohde, Problem Leader; D. A. Hanson, B. J. Newby

The greatest portion of recent laboratory effort has been devoted to studying the removal of ruthenium from simulated raw calciner off-gas by adsorption on silica gel as a function of silica gel regeneration temperature and superficial off-gas vapor velocity. In order to compare the relative ruthenium adsorption characteristics of silica gel and stainless steel, stainless steel adsorption studies were made using conditions closely approximating those used for silica gel studies.

1. Equipment and Procedure

The procedure and equipment used in these studies are essentially those used for similar work reported in IDO-14422. Calciner off-gas was generated by injecting synthetic ICPP waste into a calciner where it was evaporated at 400° C. The synthetic waste being continuously fed into the ruthenium generator had been treated with excess silver nitrate to remove traces of chloride ion. Before the silver nitrate treatment the calciner feed had consisted of:

6.6M nitric acid
0.029 g/l ruthenium as ruthenium trichloride
6×10^6 β's/(min)(ml) ruthenium trichloride tracer

Simultaneous to the feed injection, preheated air was introduced into the calciner at a rate corresponding to that of the preliminary process flowsheet. The off-gas was directed from the calciner to the appropriate ruthenium adsorbing column.

All studies involving the use of silica gel as a ruthenium adsorber were carried out in a heated straight-tube adsorbing column. The column was made of 3/4-inch stainless steel and was held in a vertical position, the off-gas entering at the bottom. The adsorption column contained about 130 cc of 6-16 mesh silica gel (91 g) which represents a bed depth of approximately 26 inches. The regeneration of silica gel was accomplished by disconnecting the column from the off-gas line; feeding 200 ml of water into the adsorption bed through the off-gas exit at a rate of 2 cc/minute (the temperature of the water was kept at 65° C), and then forcing preheated air through the bottom of the bed.

Stainless steel adsorption experiments were performed using a heated 13-1/2 and 20-inch lengths of pipe. The 13-1/2 inch pipe was 1-1/2 inches in diameter and contained about 170 g of adsorbent (23.7 cubic inches); the 20-inch pipe was a 1/2-inch pipe and contained 76 g of adsorbent (6.13 cubic inches).

In a typical experiment all of the off-gas was first directed into a pre-adsorption column caustic scrubber for 15 minutes, and then all of the off-gas was directed through the filter adsorbent media and into a post-adsorption column caustic scrubber for 45 minutes. The same technique was used for each succeeding hour of calciner operation. After each period of scrubber operation, the caustic in all scrubbers was replaced. Counting of the scrub solutions yield decontamination values.

2. Silica Gel Studies

a. Adsorption. The ability of silica gel to remove ruthenium from simulated raw calciner off-gas was studied at a superficial vapor velocity of 1.2 feet/second using an operating temperature of 100° C. A summary of the results obtained from this run (RAS-35) along with those obtained from a previously reported run (RAS-15-4) of approximately the same column ruthenium loading but at a vapor velocity of 0.6 feet/second are shown in Table VII-1. A ruthenium decontamination factor of 8000 is not necessarily significantly superior to one of 1,300; when working at low activities such a difference in ruthenium decontamination factors represents only a difference of several cts/minute in the treated gas and may only point out analytical difficulties in determining low activity in the presence of high background. Increasing the vapor velocity from 0.6 ft/second to 1.2 ft/second did not have an adverse effect on the removal of ruthenium from off-gas with silica gel. However, it was much more difficult to remove the ruthenium from the adsorbent loaded at the higher vapor velocity than the one loaded at a vapor velocity of 0.6 ft/second. In the latter case 2 columns of warm water (65° C) removed of the order of 90 percent of the ruthenium while in the former case the same volume of warm water removed less than 40 percent of the ruthenium.

Table VII-1

Ruthenium Adsorption on Silica Gel as a Function of Vapor Velocity

Run No.	Superficial Vapor Velocity (Ft/Sec)	Minutes of Successive Adsorber Operation	Ruthenium D.F.	Ru Capacity (g Ru/Ft^3)
RAS-15-4	0.6	5200	200-1,300	9.7
RAS-35	1.2	2910	350-8,000	7.2

A column activity profile of RAS-35 showed a sharp concentration gradient indicative of good adsorption performance as may be noted in Figure VII-1. Most of the ruthenium activity was adsorbed in the first fourth of filter length indicating that the column's capacity for adsorbing ruthenium had probably not yet been approached.

b. Regeneration. To make silica gel completely active again after having adsorbed water, it must be heated. There are two methods of heating usually used for regenerating silica gel; -- the static method consists of placing silica gel in an oven and heating it at temperatures between 140 to 180° C (the method used to heat the silica gel used in Run RAS-15-4); the dynamic method consists of blowing hot air over silica gel. Since the latter method would be the logical one for use in heating silica gel located in the off-gas train of the proposed ICPP calcination process, some time was devoted to ascertain the relationship existing between the regeneration temperature of a silica gel column, using the dynamic method of heating, and its ruthenium adsorption efficiency.

Heat was supplied to the silica gel bed (through which air was flowing) by externally heating the stainless steel tube containing the silica gel; a thermocouple located in the center of the bed indicated the regeneration temperature of the column except when the desired regeneration temperature was 180° C. In the latter case the temperature of the air entering the bed was 145° C. Thus, when regenerating the column at 180° C using the above procedure a small portion of the silica gel at the bottom of the column was probably regenerated at a temperature actually less than 180° C.

The same 130 cc of silica gel (bed depth approximately 26 inches) was used to make all the regeneration studies. Simulated off-gas at a superficial vapor velocity of 0.6 ft/second was directed through the silica gel bed maintained at 100° C for about 12 hours, ruthenium was removed from the bed with water, and the bed was subjected to the desired regeneration temperature and air flow overnight (in one case the regeneration consisted only of removing ruthenium with water, no heat was used). This cycle was repeated using the same silica gel but varying the method of drying the silica during regeneration. Table VII-2 summarizes the ruthenium

FIGURE VII-1

ACTIVITY CONTOUR FOR RUTHENIUM ON SILICA GEL

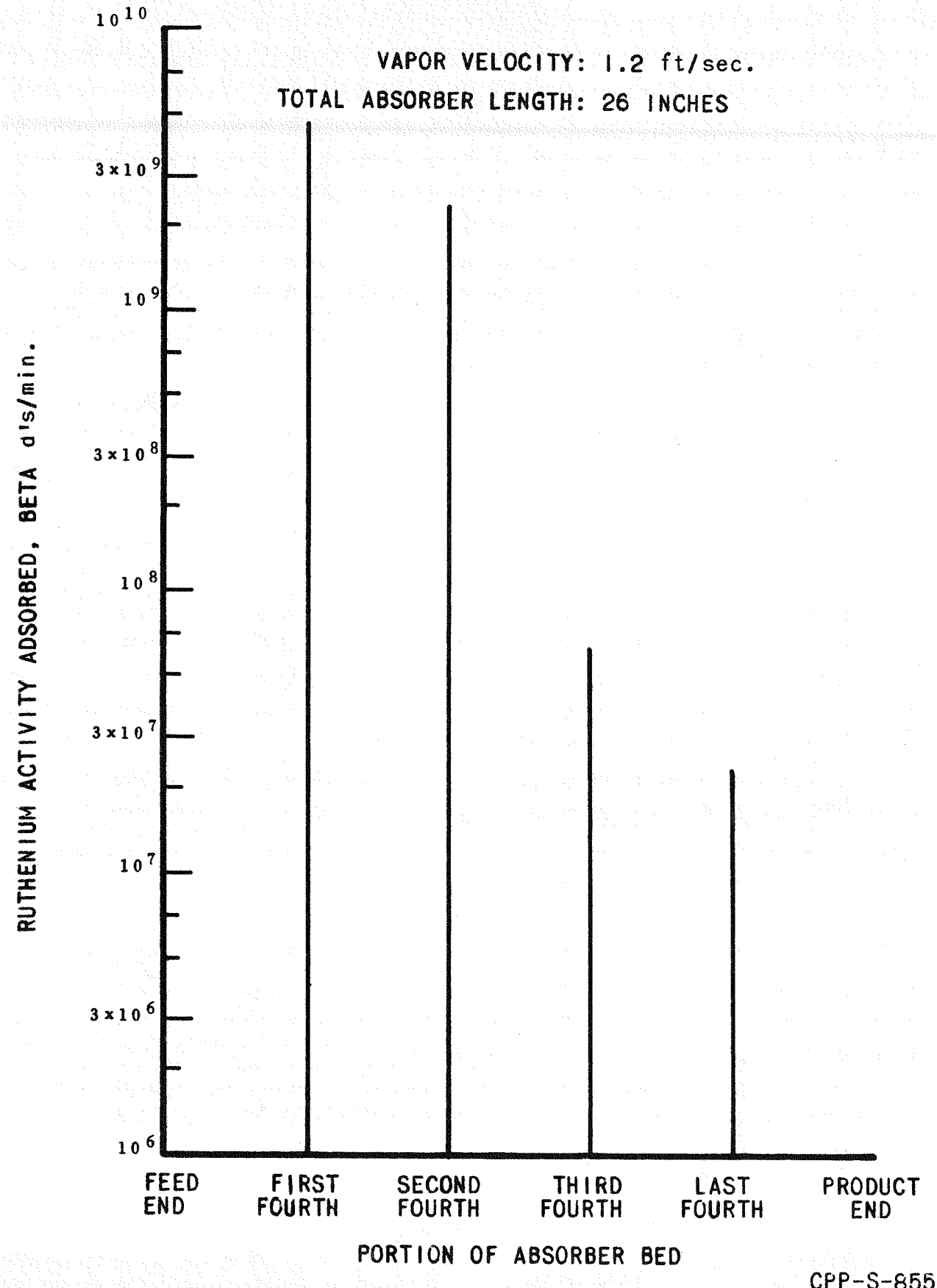

CPP-S-855

decontamination factors obtained by regenerating the column at different temperatures and air flows. The silica gel never reached its capacity for adsorbing ruthenium in these short runs. These data indicate that the peak efficiency (highest decontamination factor) for ruthenium removal from calciner off-gas by silica gel is a direct function of the silica gel regeneration temperature and air flow rate. Of the regeneration temperatures studied, air flow being constant, 180° C seems to give the best results.

Table VII-2

Ruthenium Adsorption on Silica Gel
as a Function of Regeneration Temperature and Air Flow

No. of Times Silica Gel Regenerated	Minutes of Successive Adsorber Operation	Regeneration Temperature °C	Air Flow Rate Liters/Minute	Ruthenium D.F.
New Silica Gel	720	---	---	100-35
1	720	180	11.5	150-970
2	270	180	0	75-200
3	510	Only regeneration treatment received was to remove Ru with 65° C water		70-170
4	780	100	11.5	140-360
5	720	140	11.5	125-710
6	720	180	11.5	175-1090

2. Studies with Stainless Steel

In previously reported work all ruthenium adsorption studies involving stainless steel as the ruthenium adsorber were carried out in a column consisting of three independent sections of pipe coupled together with pipe unions. When packed with stainless steel adsorbent, each pipe represented a bed depth of 4-1/2 inches. Experiments were performed using one 13-1/2 inch continuous length of Type 304 stainless steel Yorkmesh as an adsorber to indicate whether having the adsorbent in sections rather than continuous has an adverse effect on the ruthenium adsorption characteristics of stainless steel. At a superficial vapor velocity of 0.1 ft/second (bed temperature 80° C) a ruthenium capacity of 0.19 g/cu.ft. of filter was realized, the maximum ruthenium decontamination factor being 180. At higher vapor velocities much poorer results were obtained. These results are no better than the ones obtained under similar conditions using a column equivalent in length composed of three sections. Thus, a continuous column of stainless steel adsorbent offers no advantage over the sectional column.

One experiment was run using over 20 continuous inches of Type 304 stainless steel Yorkmesh as adsorbent at a superficial vapor velocity of 0.6 ft/second (bed temperature was 80° C). Since this is about the bed depth and the vapor velocity used in silica gel experiments, the experiment should compare the relative ruthenium adsorption characteristics of silica gel and stainless steel quite fairly. The experiment should also show whether increasing the depth of stainless steel adsorbent improves the adsorption properties for ruthenium. Both the ruthenium decontamination factors and the ruthenium capacity obtained in this run were poorer than those obtained in a run packed with the same adsorbent using three separate 4-1/2 inch sections at a superficial vapor velocity of 0.6 ft/second and a bed temperature of 80° C. The maximum ruthenium decontamination factor obtained in the latter run was 330 and the ruthenium capacity was 0.25 grams Ru/cubic foot of adsorber. Thus, stainless steel is a much poorer adsorber of ruthenium as compared to silica gel, and apparently increasing the depth of stainless steel adsorber does not improve adsorption.

B. Particle Removal from Calciner Off-Gas, E. S. Grimmett, Problem Leader

The purpose of this work is to develop adequate gas treating equipment to separate essentially all of the solid particles from calciner off-gas. Currently studies center around venturi scrubbers with which it is hoped to remove about 99 percent of the solids. The venturi scrubber can be followed by an AEC filter or an electrostatic precipitator to remove sub-micron particles.

1. Venturi Scrubber Tests, B. R. Wheeler

Three venturi scrubbers are being evaluated, two of which are on the pilot plant calciners. The third is an independent apparatus which is used to permit scrubbing conditions to be controlled more closely than is possible with the calciners. The scrubbing principle is that by which a rapidly moving aerosol collides with a curtain of scrub solution forming impaction surfaces for the particles in the gas. The water-solids particles are then separated by a knock-out cyclone.

a. Six-Inch Calciner Venturi Scrubber. Numerous operational difficulties which prevented calciner runs during this period also prevented further scrubber evaluation. The calciner is now being operated and the evaluation program will proceed.

In recycling scrub solution to the calciner scrubbers, the recycle pumps have been a source of trouble. The scrub solution consists of finely divided particles suspended in dilute nitric acid which erodes bearings and pump packing rapidly. A small Vanton pump has been installed to recycle scrub solution and appears to be satisfactory.

b. Two-Foot Square Calciner. The throat of the venturi scrubber on the large calciner was increased from 0.47 inches to 0.625 inches to decrease pressure drop across the scrub apparatus. A section of pipe between the venturi scrubber and the knock-down cyclone was packed with 25 inches of Yorkmesh. The Yorkmesh provides a surface upon which atomized droplets of solution from the venturi tube may coalesce. The larger sized liquid particles thus formed are easier for the cyclone to separate from gas.

c. Experimental Venturi Scrubber. The experimental scrubber set-up differs from the calciner scrubbers only in the manner of aerosol generation. The calciners generate the aerosol in the one case while a fluidized column packed with ground alumina particles is used to generate an aerosol for the experimental scrubbers. The average size of the ground alumina particles is 2.0 microns as measured by a Fischer sub-sieve sizer. The experimental venturi scrubber has a 1/4-inch diameter throat and a 2-inch length of Yorkmesh packing between the venturi and the knock-out cyclone.

Data have been taken to determine venturi scrubber performance as a function of scrub rate and aerosol velocity in the venturi throat. In the previous quarterly (IDO-14430) curves were presented which illustrate that venturi scrubber efficiency increased with increases in aerosol velocity and scrub rate at the expense of pressure drop. Some additional data at low aerosol velocities have shown that high scrub rates have less effect on the scrubber efficiency than at high aerosol velocity.

The apparatus has since been modified to include 2 venturi scrubbers in series, each of which is followed by a knock-out cyclone to separate the air from the water-solid particles. It was hoped that a higher overall gas cleanup might be achieved with a smaller overall pressure drop.

In an attempt to operate the system under vacuum to simulate proposed plant operation, lack of sufficient vacuum prevented satisfactory operation. The vacuum runs have been temporarily abandoned for operation under slight pressure. Several pressure runs have been made with the two venturis in series but the data thus far have been inconclusive.

2. Electrostatic Precipitator Studies, E. Hylsky

Work was initiated to test the use of an electrostatic precipitator on a calcination off-gas system. Several runs with the dry-type precipitator were made to become familiar with the equipment and to determine operation characteristics and efficiency. A water reservoir was then attached to the precipitator to provide a constant water flow to wash down the precipitator collecting plate. This will be used to test efficiency in extended runs. Dust generating and metering equipment was constructed to provide a source of a typical aerosol.

C. Heat Supply for Scale-Up Calciner, E. S. Grimmett, Problem Leader, G. E. Lohse

Three different methods are being utilized for supplying heat to the scale-up (100 liter per hour) calciner. They are: (1) electrical heaters placed directly in the fluidized bed, (2) high temperature NaK pumped through coils placed in the calciner bed, and (3) high temperature combustion gases forced at high velocity through coils placed in the calciner bed.

Electrical heaters have been used exclusively in the small 6-inch calciner and a few tests have been made in the large calciner using electrical heaters. As a heat source for radioactive operations, electrical heaters have a significant probability of failure if the rate of heat transfer between the heater and the bed momentarily becomes low. This has been observed in both the small and the large calciners.

A NaK heat transfer loop has been chosen as the primary source of heat for the large calciner. Heat transfer is high, no local hot spots can develop in the calciner exchange bundle and control of a wide range of heat loads is possible. A rupture or leak in the tube bundle which would allow NaK to leak into the calciner would result in serious damage to the calcining equipment. This is a serious disadvantage and therefore a safer system would be desired.

Direct fired tubes as normally utilized have the disadvantage of a low heat transfer coefficient on the gas side of the tube. This is because insufficient pressure is available from the burner to force the hot gases through the tubes at the high velocities needed for more efficient transfer. If reasonable heat transfer rates could be achieved with such a system, however, the danger of leaks or ruptures in the tubes would be much less than those associated with the NaK system. Tests have been made on a higher pressure fired-tube system to obtain a preliminary evaluation of feasibility.

1. Heat Transfer Measurements with Direct Fired Tubes

The high mass flow rates required of the combustion gases in the tubes of the calciner heat exchanger in order to obtain reasonable heat transfer coefficients cannot be obtained unless these gases are available at a significant pressure (5 to 10 psig). Since a standard burner will not operate at these pressures, an oil burner was designed to deliver hot combustion gases at pressures up to 30 psig. This burner was designed similar to the burners used in aircraft turbojet engines where pressures as high as 45 psig and up are used. Figure VII-2 shows a schematic drawing of this burner.

The heat exchanger bundle used in the calciner was constructed of 6 parallel Type 316 stainless steel tubes welded into headers at the top

FIGURE VII-2
OIL BURNER FOR PRESSURE OPERATION

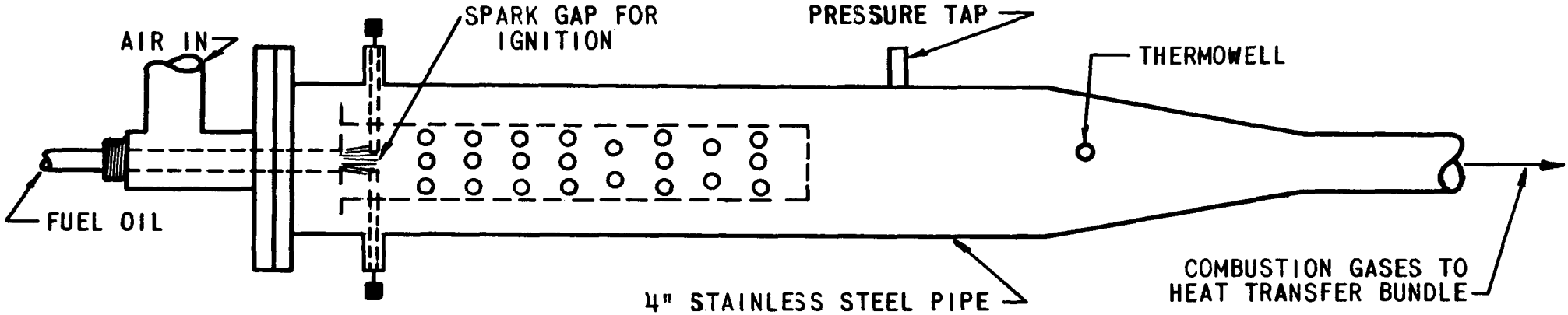

CPP-S-656

and the bottom of the bundle. Each tube was 8.6 feet long by 3/4 inches in diameter, with a wall thickness of 0.065 inches. The available heat transfer area, based on the bed side, was 10 square feet. The burner and the heat exchanger were mounted on the calciner as shown in Figure VII-3.

Nominal gas temperatures were measured by thermocouples at the burner exit, at inlets and outlets of three of the tubes, and in the outlet manifold. It was not attempted to shield the thermocouples from radiation losses because of the short time available for making the installation, and estimation of the radiation correction was not possible lacking information on wall temperatures. For each of three tubes, an outer wall temperature was measured by a thermocouple located about midway of its length. Bed temperature thermocouples were provided both above and below the tube bundle.

Part of the gas leaving the heat exchanger was used to supply fluidizing air. This system was unsatisfactory since the fluidizing air requirement affected the vent line back pressure and burner conditions.

Rough estimates of overall and film coefficients were made by calculations based on the following assumptions:

1. Coefficient constant over length of tube.

2. Specific heat of combustion gases equal to that of air (it was estimated that this would result in a coefficient which was 2-5 percent low).

3. Combustion was complete at tube entrance (this appeared to be a significant error as in some cases apparent tube wall temperatures were higher than calculated gas temperatures).

Overall coefficients of the order of 10-30 were noted as shown in a summary of these data given in Table VII-3. The data show large variations and are not consistent in that the apparent overall coefficient for the bundle was generally greater than that for the tubes on which data were available. Although the largest overall coefficient was obtained for the highest mass flow rate, there was otherwise no apparent correlation between gas flow and transfer rate for either inner film or overall transfer rates. Significant and generally consistent differences were noted among the individual tubes, which may reflect either unequal flow distribution or differences only in temperature measurement errors. The apparent coefficients from tubes to bed also showed large and erratic variations.

An additional discrepancy was noted in that for some cases the amount of heat transferred, based on calculations using overall coefficients for individual tubes, was insufficient to heat, evaporate, and decompose the amount of feed which was actually undergoing conversion. This also indicates significant errors in assumptions of measurements, although in a direction which suggests that the actual coefficients were larger than the estimated values.

FIGURE VII-3
INSTALLATION OF BURNER AND TUBE BUNDLE
FOR FIRED-TUBE TESTS

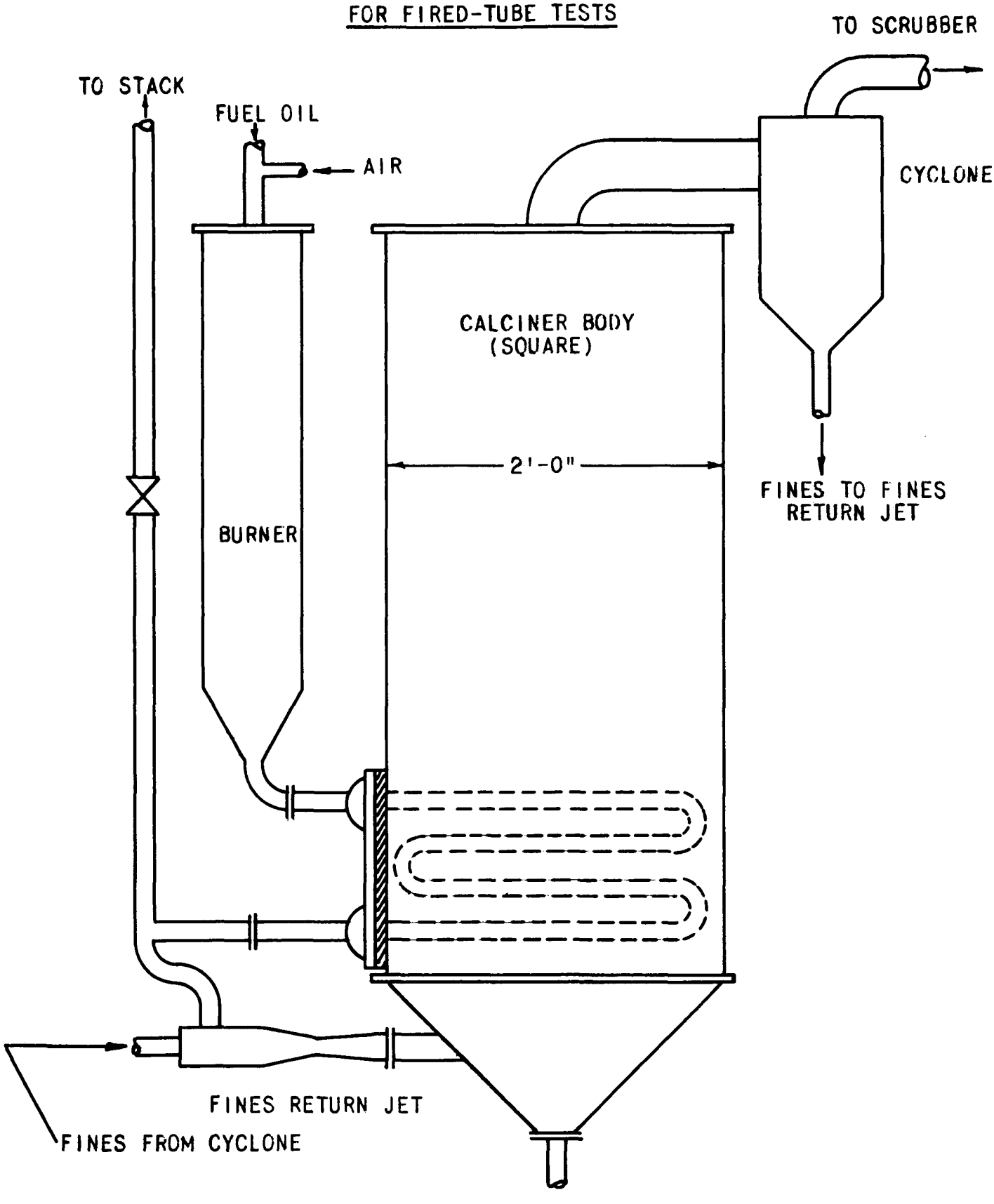

CPP-S-857

Table VII-3

Summary of Heat Transfer Data - Direct Fired Tubes

Mass Flow Rate of Burner Gas, Lbs/(Hr)(Ft^2)	Tube Bundle Pressure Drop, in Hg	Calciner Liquid Feed Rate, Liters/Hr	Approximate Calculated Heat Transfer Coefficients, Btu/(Hr)(Ft^2)(°F)							
			for Overall Bundle	Overall Coefficients			Inside Film		Outside Film	
				Tube 2	Tube 4	Tube 6	Tube 2	Tube 6	Tube 2	Tube 6
44000	14.6	16	34	10	22	--	100	--	12	--
44000	15.2	17	28	11	22	16	78	13	37	30
43000	14.8	--	14	7	14	20	126	20	7	--
53000	--	0	--	27	27	22	47	31	99	280
53000	--	0	--	15	23	18	22	--	42	18
53000	--	30	24	11	19	13	19	--	31	12
67000	20.0	23	52	15	28	21	140	54	19	40

In general, the results of these tests only indicated that direct firing of bed tubes is not infeasible, and that a much more refined measuring technique would be required to secure reliable data. It is obvious that heat transfer by this means would be limited by allowable tube temperature limits for useable materials. No attempt has been made to investigate such materials.

Further runs are planned in which the combustion gases in the tubes will be metered separately from the fluidizing air. Additional thermocouples will be placed on the bed side of the tubes so that radiation corrections can be applied to the measured gas temperatures.

2. NaK Heating System

All the components for the liquid metal heat transfer system for the large calciner have arrived. Installation of the heating components was begun and is approximately 90 percent complete. Layout drawings of the NaK loop were completed and fabrication of the components was initiated.

Discussion of liquid metal loops with ANL personnel resulted in changes in the original layouts. The surge tank will be connected to the suction side of the electromagnetic pump instead of to the line at the discharge of the furnace. A forced circulation cold trap will not be used. The existing cold trap will be installed to act as a cold finger. Incorporation of other items such as improved pressure measuring instruments, plugging indicators, liquid level indicators, etc., will be postponed at present because of anticipated prolonged delays in the procurement of these items.

D. Studies Related to Storage of Alumina, B. M. Legler, Problem Leader; P. N. Kelly

1. Thermal Conductivity of Alumina

Results obtained with the cylindrical thermal conductivity test apparatus duplicated previous results for the heat conductivity of alumina obtained with a spherical apparatus. Conductivity of calcined alumina varies linearly from 0.08 Btu/(hr)(°F)(ft) at 1000° F to 0.26 Btu/(hr)(°F)(ft) at 1800° F. Some tests have yielded apparent conductivity values up to 0.30 at 1800° F. Temperature range extension has been unsuccessful due to heating element and lead wire failure. Attempts to obtain conductivity data above 2000° F. are continuing.

2. Alumina Attrition Test

Recirculation of alumina in storage offers the possibility of improving heat removal. Air lifting could provide a nonmechanical means of recirculation. An air lift recirculation test apparatus has been operated 3840 hours to determine attrition rate of calcined alumina. At a bed turnover rate of once per hour, the percentage of fines smaller

than 60 mesh increased from 2.5 to 16.8 during the test period. This increase virtually eliminates consideration of calcine recirculation in storage as production of fine particles would require an elaborate means for particle removal prior to venting the air used for recirculation.

E. Leaching Fission Products from Calcined Alumina

Studies of the leaching of fission products and other radioactive contaminants from alumina produced by fluid bed decomposition of aluminum nitrate are being conducted to determine effects of ground waste contact, to establish means of reducing the need for removing heat from alumina in storage, and to determine if useful fission products may be recovered by this means. The solubility of fine alumina in nitric acid was measured and the stage efficiency of a multistage contactor was evaluated with Dowex-50 ion exchange resin.

1. Laboratory Studies of Fission Product Behavior, D. W. Rhodes, Problem Leader; M. E. McLain, D. R. Anderson

Preliminary equilibrium experiments with solutions, which were prepared to simulate leachate from treating calcined alumina, indicated that Duolite C-3 cation exchange resin in the sodium form may have application to the removal of radioisotopes from such solutions. The equilibrium distribution coefficient for cesium-137 in this system was determined to be approximately 90 at 25° C.

Laboratory experiments were conducted to measure the solubility of calcined alumina fines in nitric acid. A substantial portion of the alumina was readily dissolved and these data indicate to some extent the possible fate of calcined alumina particles which may be transported to nitric acid scrubber solutions by the air flowing through a fluidized bed calciner. The results of one laboratory experiment using alumina particles less than 0.150 mm diameter are shown in Table VII-4.

These data together with X-ray diffraction measurements of the alumina residues and of alumina before treatment with nitric acid indicated that the amorphous fraction was easily dissolved until the solubility limit of aluminum nitrate in nitric acid (Sample No. 1) was approached. The crystalline fraction, which was determined to be alpha alumina, was only very slightly soluble in nitric acid.

Additional ignition experiments with radioactive alumina calcined at 400 and 500° C indicated that approximately 40 to 50 percent of the cesium-137 was lost on heating at 1000° C for 18 hours. These data agree with a previous experiment in which measurements indicated that cesium-137 volatilized from calcined alumina between 800 and 1100° C.

Table VII-4

Solubility of Calcined Alumina Fines in Nitric Acid

Alumina particles (diameter less than 0.15 mm)
produced by calcining at 400° C
Nitric acid concentration: 8N
Temperature: 70° C
Contact time: 2 hours

Sample Number	Ml Nitric Acid per Gram of Alumina	Aluminum in Solution Grams/Liter (as Al)	Total Aluminum Dissolved Weight Percent (as Al)
1	5	73.3	69.1
2	15	26.7	75.4
3	30	13.4	75.7
4	150	2.7	76.3

2. Leaching Contactor Studies, B. M. Legler, Problem Leader; P. N. Kelly

Leaching of waste calcine may be desired for one or more of the following reasons: (1) removal of long-lived fission products, (2) removal of high heat-producing (short-lived) fission products, (3) recovery of fission products for sale, and (4) removal of corrosion producing nitrates.

A pulsed multistage contactor, shown in Figure VII-4, is being tested for continuous leaching of calcine. To assist in contactor evaluation, several ion exchange runs were made using 0.1N copper sulfate and Dowex-50 resin. In one series of runs the contactor was arranged as shown in Figure VII-4. In another series of runs, additional liquid-solids contact was obtained with an air lift slurry removal system. At solution mass flow rates of 1000 to 1500 lb/(hr)(ft^2) and a resin flow of 25 lb/(hr)(ft), individual tray efficiencies ranged from 30 to 40 percent. Typical operation is depicted graphically in Figure VII-5.

F. Process Design for Waste Calcination, J. I. Stevens, Problem Leader; D. K. MacQueen, R. S. P'Pool

1. Preliminary Design

A preliminary design for the demonstrational unit has been submitted by the architect-engineer (The Fluor Corporation). A thorough analysis of this design is currently in progress.

FIGURE VII-4
PULSED MULTISTAGE SOLIDS CONTACTOR

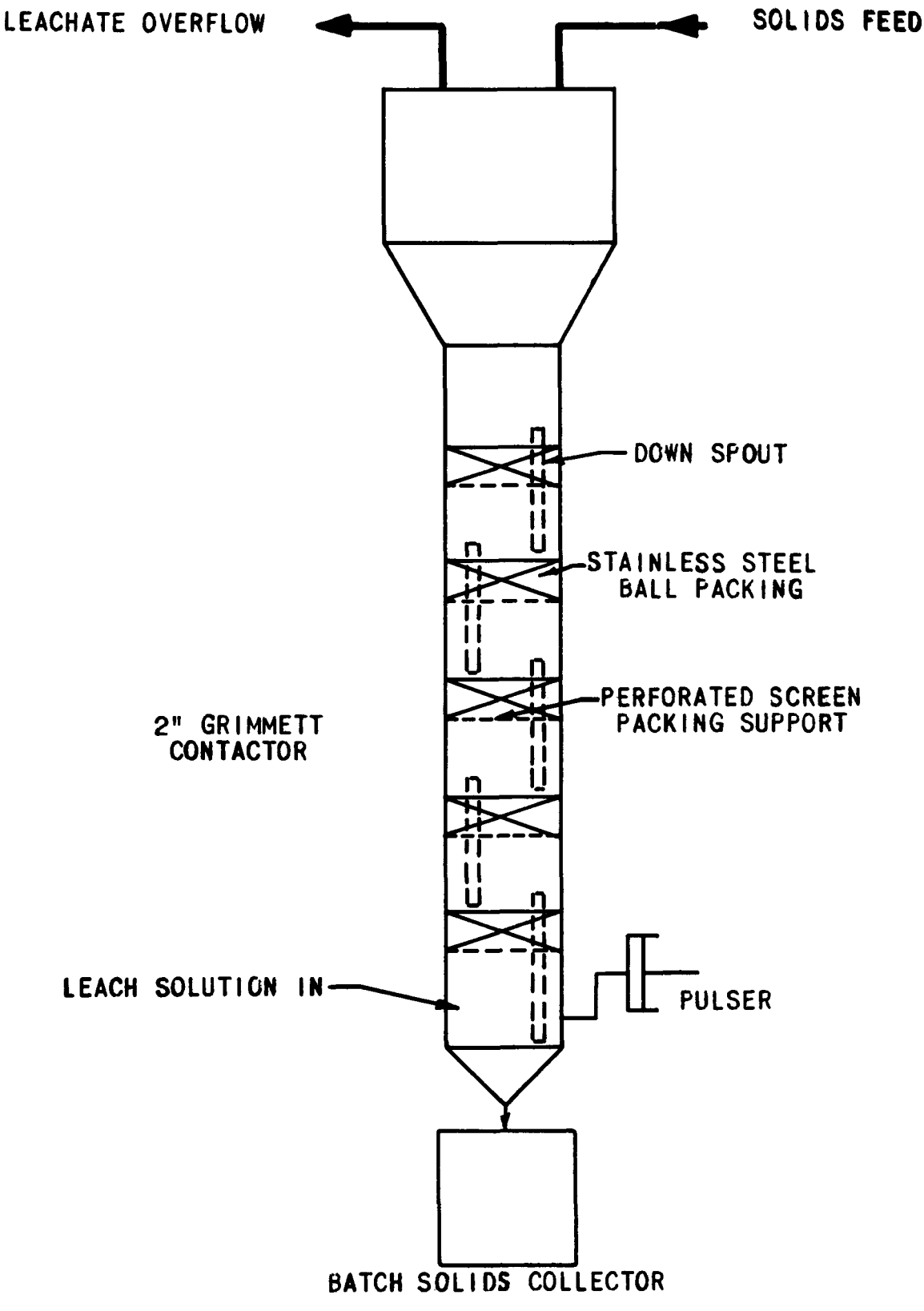

CPP-S-858

FIGURE VII-5
MULTISTAGE CONTACTOR PERFORMANCE
IN CUPRIC ION-DOWEX 50 EXCHANGE

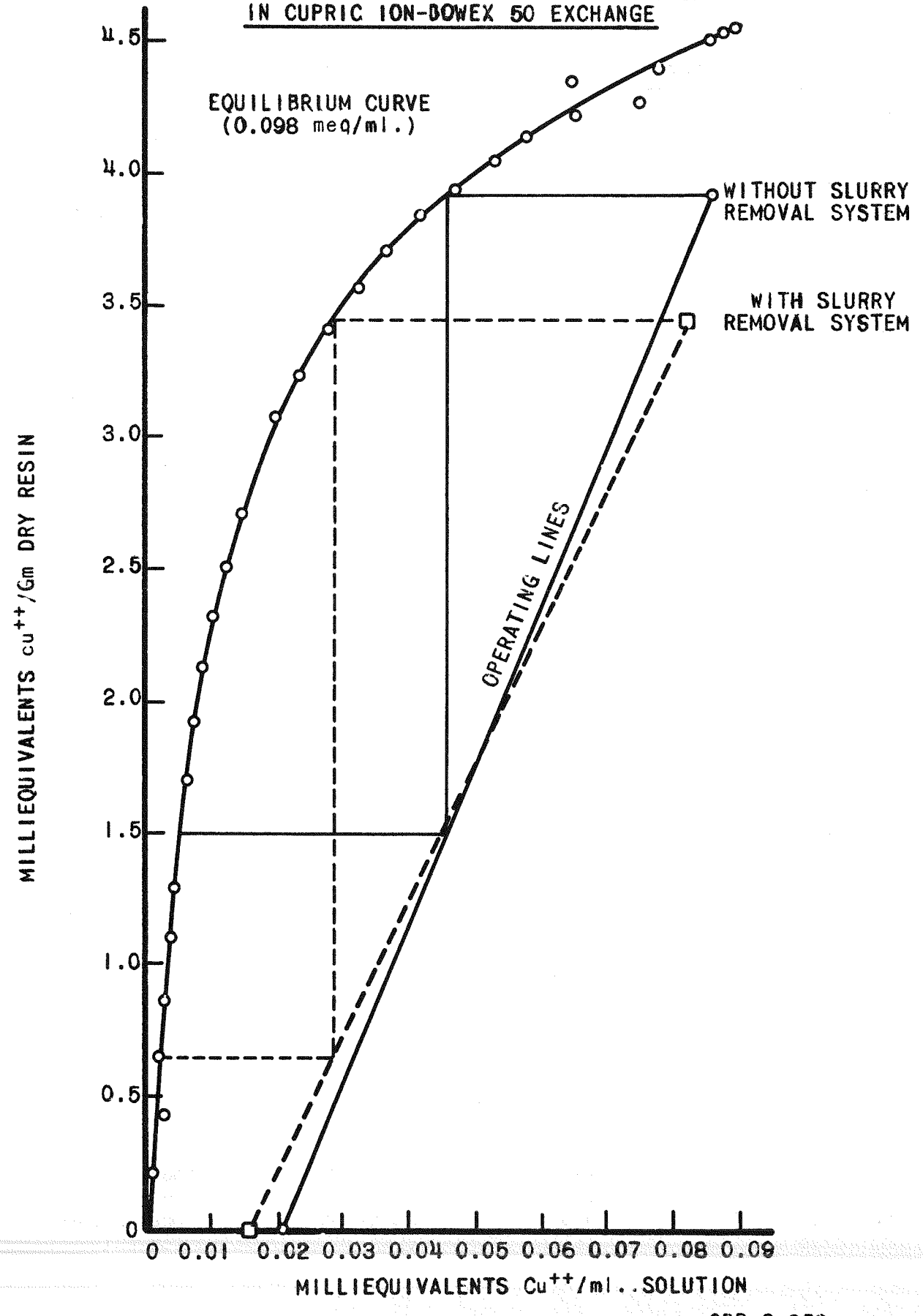

CPP-S-859

An abbreviated flowsheet of the current design is shown in Figure VII-6. The major changes that have been made in this flowsheet as compared with that planned previously are a reduction in the design feed rate to 60 gallons per hour, and elimination of the leaching and demonstration storage units. These changes reflect the plan to operate with the minimum capacity for an adequate demonstrational unit and provide for later addition of demonstrational storage as required data are developed.

The calciner will be designed to operate at 400° C, with the provision that, by a reduction in feed rate, the operating temperature can be increased to 500° C. This uncertainty in the calcination temperature results from the lack of conclusive data concerning the behavior of ruthenium in the system. ANL data indicate that ruthenium decontamination of the off-gas may be significantly improved by higher calciner operating temperatures. The primary cyclone has been changed from an internal, dip-leg unit to an external, and probably series, unit. This change was made to permit use of higher efficiency cyclones. The desirability of returning the fines collected in the primary cyclone to the bed is still open to question. In the absence of conclusive pilot plant data, provision will be made for either returning the fines or removing them from the system.

No significant changes have been made in the primary quench or venturi scrubber units. The underflow from these units will be collected in a single vessel and recirculated. The net make of liquid, resulting from the condensation of moisture in the cooled off-gas, will be returned to the calciner or a small stream will be returned to the process equipment waste system of the plant. This return stream will maintain the dissolved solids content of the circulating liquid below the solubility limit. The design efficiency of the venturi scrubber has been set at a minimum of 96 percent.

Sufficient laboratory and pilot plant data have become available to permit selection of silica gel as the best adsorbent for the ruthenium adsorber. The better mechanical stability of stainless steel does not appear to compensate for the higher efficiency and capacity of silica gel. Manifolding will permit operation of adsorbers in parallel or series. Tests are continuing to determine the optimum regeneration system. The primary problem associated with the design of the final filters is the selection of units with the required efficiency and operability. The filters must be efficient enough to provide the necessary decontamination, but the service life of the filter elements must be of reasonable length. Changing of the filter elements and disposal of the loaded elements could become a serious problem.

Preliminary design studies are being made of alternative off-gas cleaning devices. Electrostatic precipitators, moving bed filters, bag filters, and fume scrubbers are currently under study. One or more of these units may be installed if operation of the calcination unit

PRELIMINARY PROCESS FLOWSHEET FOR WASTE CALCINATION DEMONSTRATION PLANT

Figure VII-6

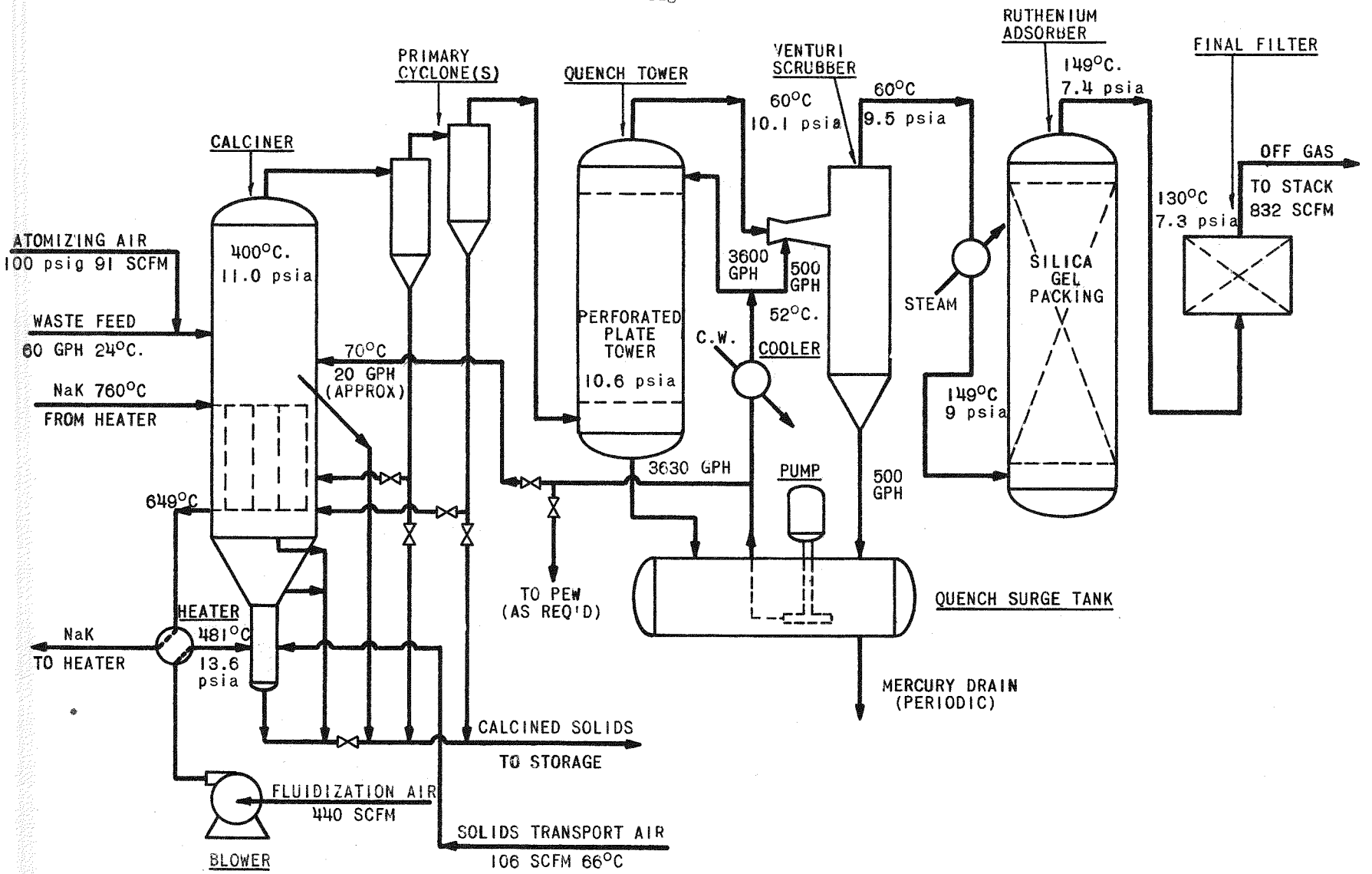

indicates their need. Consideration is also being given to replacement of the NaK heating system with electrical resistance units. A design study by the architect-engineer indicated an economic advantage for the electrical system. The major drawback to use of an electrical heating system is the uncertain service life of the heating elements, since remote replacement of defective elements would be extremely difficult.

2. Off-Gas Cleaning

Design limitations on radioactivity emitted from the waste calcination plant have been tentatively established as follows: (1) the concentration of strontium-90 in air at the ICPP perimeter fence should not at any time exceed 2×10^{-10} μc/ml., and (2) a dilution factor of 10,000 will exist between the stack and the point of exposure at the ground.

With the assumption that strontium-90 constitutes the controlling source of physiological exposure and recognizing that extenuating circumstances beyond the designer's control may make modification of these limits mandatory, calculations have been made as to the probable magnitude of the gas cleaning that must be achieved. It can be shown that with dilution air limited to the volume of calciner building ventilating air the solids loading of the off-gases before emission must be approximately 100-fold less than normal atmospheric dust loadings.

The above design limitations do not include contributions of fission products other than strontium-90. Since particles probably will contain the entire spectrum of fission products it is conceivable that a reduction in one or both of the above criteria would be required due to additive effects. For example, if waste produced from processing fuels at 200-day post reactor discharge are to be calcined it is estimated that cerium-144 would be at 47 percent of its MPC when the MPC of strontium-90 is reached.

When using demonstrated dust loadings from pilot plant equipment in conjunction with reported efficiencies for AEC filters in the sub-micron range, it is estimated that a satisfactory cleanup of the off-gas can probably be achieved. Indeed, this facility should provide an excellent means of testing the efficiency of gas cleaning equipment for removing particles in the sub-micron region, which region is always subject to analytical difficulties.

A major unknown will be the frequency of filter changes which may determine the long-term operating capabilities of the facilities.

VIII. AQUEOUS METHODS FOR WASTE TREATMENT

D. W. Rhodes, Problem Leader

Studies have been made of precipitating and extracting aluminum from aluminum nitrate waste solutions, and of gelling zirconium waste solutions containing nitric acid and fluoride with sodium silicate.

A. Aluminum Wastes, M. E. McLain, D. R. Anderson

Preliminary experiments indicated that aluminum was precipitated from aluminum nitrate solutions when sodium silicate solution was added. More detailed laboratory investigations indicated that the precipitate was actually a mixture of aluminum hydroxide and silica rather than aluminosilicate. Leaching the precipitate with water did not remove fission products adequately, and a dilute acid leach dissolved the aluminum hydroxide.

Additional probing experiments indicated that aluminum could be precipitated quantitatively as aluminum phosphate from dilute aluminum nitrate solution (0.5M). The precipitate formed slowly when urea hydrolysis was used to raise the pH of the solution. The resulting precipitate settled rapidly and was easily filtered. Some excess phosphate in addition to that required to precipitate aluminum as $AlPO_4$ appeared to be necessary to produce a granular precipitate. Optimum conditions for the precipitation, and the distribution of fission products in the system are yet to be established.

Experiments using acetylacetone in carbon tetrachloride indicated that aluminum could be readily extracted at 25° C from dilute aluminum nitrate solutions (0.25M) when partially buffered with ammonium acetate. At pH values greater than 4.0, a precipitate of aluminum acetylacetonate formed, which was soluble in excess acetylacetone. Thus, under controlled conditions, the reaction between aluminum in solution and acetylacetone might be used to remove aluminum either by solvent extraction or precipitation. Investigations to define better the optimum conditions for the separation of aluminum from fission products by acetylacetone extraction are continuing.

B. Solidification of Aqueous Wastes, D. R. Anderson

Preliminary laboratory investigations indicated that a zirconium waste solution, which was approximately 1M hydrofluoric acid, 1M zirconium, and 7M nitric acid, could be mixed with an equal volume of sodium silicate solution (one volume of 40° Be' sodium silicate to one volume water) to form a firm, hard gel. The gel was easily extruded through a wire screen to form granules, and preliminary observations indicated that mixing the gel granules with calcium carbonate for storage may repress the loss of liquid from the granules due to syneresis of the gel. Additional investigations are planned to attempt to adapt this or similar procedures to the disposal of bulk zirconium wastes, which have been separated from the gross fission products by a previous treatment.

IX. ANALYTICAL METHODS DEVELOPMENT

R. C. Shank, Section Head

The distribution of neptunium isotopes was determined mass spectrometrically in a special sample, using a surface ionization instrument, and boron in polyethylene was determined with a Consolidated spectrometer. Uranium emission spectra from a hollow cathode tube were studied. A method for the determination of tin by tetrabromide distillation and amperometric titration was developed. Other chemical methods studied involved the determination of nitrate, nitrite, copper, fluoride, and neptunium.

A. Spectral Analysis, T. D. Morgan, Problem Leader

1. Surface Ionization Mass Spectrometers, P. Goris

An isotope distribution analysis was attempted on neptunium-237 at the request of the Nuclear Physics Group at MTR for use in cross section studies. Ion beams were observed in mass regions corresponding to Np^+, NpO^+ and NpO_2^+ with relative intensities of 1, 3×10^4 and 4×10^4, respectively. The neptunium was identified as principally neptunium-237. A small peak at the neptunium-236 position may have been caused by approximately 0.02 percent neptunium-236. Further identification work on this peak is planned.

2. Consolidated Mass Spectrometer, R. M. Abernathey

A method was developed for measuring isotopic ratios of milligram quantities of boron in polyethylene tape. It was necessary to separate the boron from the polyethylene and prepare a volatile derivative. The tape was distilled off and the boron converted to methyl borate, which was introduced into the mass spectrometer as a gas. The mass spectrometer gas inlet system was flushed with methanol vapor between analyses to reduce memory effects.

3. Emission Spectrograph, G. V. Wheeler

Consistently satisfactory excitation of uranium spectra in a hollow cathode tube has been achieved. Cathode length and diameter, gas pressure and sample preparation have all proven to be critical for good results. Conditions for satisfactory excitation were established, though not optimized, and the spectra obtained exhibit a definite improvement in line sharpness over arc spectra. The full extent of the improved resolution thus obtained cannot be established here due to the limited resolution of the present spectrograph.

B. Analytical Development (Chemical Methods), J. E. Rein, Problem Leader; G. L. Booman, Assistant Problem Leader

1. Determination of Tin, S. S. Yamamura

A specific method has been developed for the determination of tin. It is based on distillation of tin tetrabromide followed by an amperometric titration with cupferron in a strong acid electrolyte. The distillation is made with a 1 to 3 mixture of hydrobromic acid-hydrochloric acid from a sulfuric acid media at 155 to 165° C. Because bromide and chloride interfere in the cupferron titration, the distilled tin is separated by precipitating with ammonia with aluminum hydroxide carrying. The precipitate is dissolved with 10M sulfuric acid, adjusted to 2M in sulfuric acid and 3M in ammonium sulfate, and titrated with cupferron at -0.84 volts against a saturated calomel electrode. Ten mole ratios and greater of copper, iron, niobium, molybdenum, titanium, and tungsten do not interfere. Zirconium at a mole ratio of 100 to 1 does not interfere making the method especially attractive for the determination of tin in zirconium base alloys like Zircaloy, a popular fuel element material.

Under the conditions above, the only interferences are bismuth and antimony. Antimony can be preseparated by distilling it as the chloride from sulfuric acid. By adding phosphate and distilling tin tetrabromide at a lower temperature (135 to 145° C), no bismuth is carried along.

Precision of the method is better than one percent coefficient of variation for a single determination.

2. Determination of Nitrite, B. E. Paige

A spectrophotometric method based on that of Brouns[10] was developed for the determination of nitrite in calcined aluminum nitrate waste stream samples. The sample is dissolved with hot 15M sodium hydroxide. A volume aliquot is then treated with Amino G (7-amino-1, 3-naphthylanimdedisulfonic acid) which reacts with the nitrite to form a diazonium salt. The salt is then coupled with α-naphthylamine to form an intensely colored aminoazo compound with an absorbance peak at 545 mμ. A monochloracetate buffer system at pH 2.6 is used for color development. After color development is complete (in 15 minutes), sulfuric acid is added to dissolve the partially precipitated aluminum hydroxide and the solution is left for 30 minutes, then diluted to volume.

The molar absorptivity is 36,800. The absorbance response is linear for the range of 1 to 4 micrograms of nitrite in the final 25-ml volume with 5-cm cells. The lower limit corresponds to 10 micrograms of nitrite per gram of calcined sample.

(10) Brouns, R. J., Hanford Atomic Products Operation, Private communication to J. E. Rein, April 1, 1957.

3. Determination of Neptunium, W. J. Maeck

A radiochemical method based on that of Moore[11] was developed for the determination of neptunium in plant aqueous samples. A 2-cycle extraction system using thenoyltrifluoroacetone in xylene as the extractant and controlled oxidation-reduction conditions gave over 95 percent recovery of neptunium and but 0.005 percent recovery of plutonium. This corresponded to greater than 19 alpha counts of neptunium per count of plutonium. A series of plant samples was analyzed which indicated that the neptunium was being recycled in the TBP first cycle process by accompanying the second cycle raffinate.

4. Determination of Copper, S. S. Yamamura

A series of samples originating from an ion exchange equilibrium study and containing variable ratios of copper and sodium was received for copper analysis. A direct ethylenediamine tetraacetic acid titration at pH 10 to a color end point with murexide was found to be satisfactory.

5. Determination of Fluoride, R. W. Henry

An ORNL pyrolysis method was modified for the determination of fluoride in zirconium samples. In this method, moisture-saturated air is passed over the sample in a platinum boat in a quartz tube furnace. As the temperature is raised (from 300 to about 800° C), hydrofluoric acid is evolved which is continuously titrated with standard base to a phenolphthalein end point. Samples that contain other anions in addition to fluoride are titrated with thorium nitrate to a conductometric end point.

A statistical analysis, based on a series of standards and duplicate samples, indicated that there was no significant difference of precision between standards and samples for either mode of titration and no significant difference of bias between the two modes of titration (for samples containing only fluoride). The standard deviation of the entire method for the average of duplicates is 0.9 percent when the alkalimetric titration is used and 2.5 percent when the conductometric method is used.

6. Determination of Nitrate, B. E. Paige

A colorimetric method has been developed for small amounts of nitrate in aqueous solutions containing zirconium and fluoride. Involved is addition of caustic, evaporation to dryness, and addition of phenoldisulfonic acid in sulfuric acid, which is nitrated. The solution is then made basic with potassium hydroxide and the absorbance of the yellow complex is measured at 407 mμ. The hydrous oxides of any cations that form are separated by centrifugation. The only known interferences are chloride and carbonate which cause a loss of nitrate.

A mole ratio of zirconium-to-nitrate of 15 : 1 and of 1 : 2 for uranium can be tolerated. With 5-cm cells and a 1-ml aliquot, the lower limit is 0.005M nitrate in the original sample.

(11)Moore, F. L., Anal. Chem. 29, 941 (1957)